Holocene Glacial History of the Bowser River Watershed, Northern Coast Mountains, British Columbia

by

Vikki Maria St-Hilaire
Bachelor of Science, University of Northern British Columbia, 2011

A Thesis Submitted in Partial Fulfillment
of the Requirements for the Degree of

MASTER OF SCIENCE

in the Geography

Supervisory Committee

Glacial History of the Bowser River Watershed,
Northern Coast Mountains, British Columbia

by

Vikki Maria St-Hilaire
Bachelor of Science, University of Northern British Columbia, 2011

Supervisory Committee

Dan J. Smith (Department of Geography, University of Victoria)
Supervisor

John J. Clague (Department of Geography, University of Victoria)
Departmental Member

Abstract

Supervisory Committee

Dan J. Smith (Department of Geography, University of Victoria)
Supervisor

John J. Clague (Department of Geography, University of Victoria)
Departmental Member

Accelerated glacial recession and downwasting of glaciers in the Bowser River Watershed of the northern British Columbia Coast Mountains have exposed subfossil wood remains and laterally contiguous wood mat layers. To develop an understanding of Holocene glacial fluctuations in this region, field investigations were conducted in 2005, 2006 and 2013 at Frank Mackie, Charlie, Salmon and Canoe glaciers. These wood remains represent periods of Holocene glacier advance, when glaciers expanded and overwhelmed downvalley forests.

Dendroglaciology and radiocarbon analyses revealed five intervals of glacial expansion: (1) a mid-Holocene advance at 5.7-5.1 ka cal. yr BP; (2) an early Tiedemann advance at 3.6-3.4 ka cal. yr BP; (3) a late Tiedemann advance at 2.7-2.4 ka cal. yr BP; (4) a First Millennium AD Advance at 1.8-1.6 ka cal. yr BP; and, (5) three advances during the Little Ice Age at 0.9-0.7, 0.5 and 0.2-0.1 ka cal. yr BP. These results provide new evidence for mid-Holocene glacier activity in northern British Columbia, as well as supporting previous research that Holocene glacier advances were episodic and regionally synchronous.

Table of Contents

List of Tables

List of Figures

Acknowledgments

Endless thanks to my supervisor, Dr. Dan Smith for supporting this research, bringing me into the field and letting me be part of the UVTRL during the past two years. I have been very fortunate to have a supervisor who gave me the freedom to explore on my own, but whose door is always open to questions and edits. Thank you for bringing me along to experience some of the most remote areas of British Columbia! I will always remember the glow of Franklin Glacier under the full moon and that mountain goat galloping full speed across the ice.

Thank you to Ansley Charbonneau and Bryan Mood for being my field assistants and stuffing their packs full of wet, muddy samples. Thank you to Jess Craig for teaching me how to prepare my samples and to Jill Harvey for teaching me how to analyze them. Thank you to Bethany Coulthard for her joyfulness in the lab. Thank you to Jodi and Peter for always welcoming us to their home in the Cariboo on our way to and from fieldwork. And thank you to Cedar Welsch for making me the tastiest birthday pancakes one could ever imagine in the field.

I am grateful to my committee member, Dr. John Clague for his insights and enthusiasm on the Bowser Watershed glaciers. Thank you for Dr. Alberto Reyes for acting as external and leaving me with me with plenty of feedback to help improve this thesis.

Thank you to my family, especially my mom, for instilling the value of post-secondary education. Thanks to Dar Purewall for first asking me whether I was going to do a graduate program, long before I ever I thought about it myself, and thanks to Rowland Atkinson for convincing me to start one now as the money will be there waiting for me later.

Finally thank you to Ryan Weston, for always being there to support and encourage me, and for your endless love. Without you, I'm just V.

Chapter 1: Introduction

Glaciers worldwide have been retreating during the past century in response to a warming climate, initiated at the end of the Little Ice Age (LIA) (Dyurgerov and Meier, 2000; Dyurgerov and McCabe, 2006). The loss of glacier mass has numerous ramifications at global, regional and local scales. Implications include a rising eustatic sea level, possible disruption of the timing of flow and/or volume of water resources required by communities and industries, as well as effects on tourism and recreational opportunities (Barry, 2006).

Recent glacial retreat, however, provides us with an opportunity to learn about the past environment through clues previously buried or disturbed by glaciers. As glaciers retreat, slopes are destabilized and experience deformation, rock avalanches, debris flows and slides (Holm et al., 2004). As slope material is removed, evidence such as stratigraphic records and organic material become accessible, and can be analyzed and dated. Previously buried trees can be dated using dendrochronological techniques or radiometric dating, and used to reconstruct periods of glacier advance and retreat during the Holocene. Reconstruction takes into consideration spatial and temporal patterns of climate forcing mechanisms. The resulting glacier and climatic reconstruction and understanding of these influencing patterns are necessary inputs for producing models to predict future climate change (Winkler and Matthews, 2010).

Glaciers in Alaska and British Columbia (BC) have been found to be sensitive to climate variability (Larsen et al., 2007) and, therefore, determining periods of

glacier advance and retreat provides proxy information for inferring climate in the region beyond the instrumental climate record. Research on the northern Coast Mountains' glacier history remains fairly limited despite the presence of approximately 3000 glaciers occupying a total area of 8549 km^2 (Schiefer et al., 2008). Opportunities for research have been constrained by issues of accessibility, owing to both the remoteness of many potential study sites and the long snow cover season. One of these remote sites, the Bowser River Watershed, has been selected as the field site for this study to build a more robust record of Holocene glaciological and climatology history for northern BC.

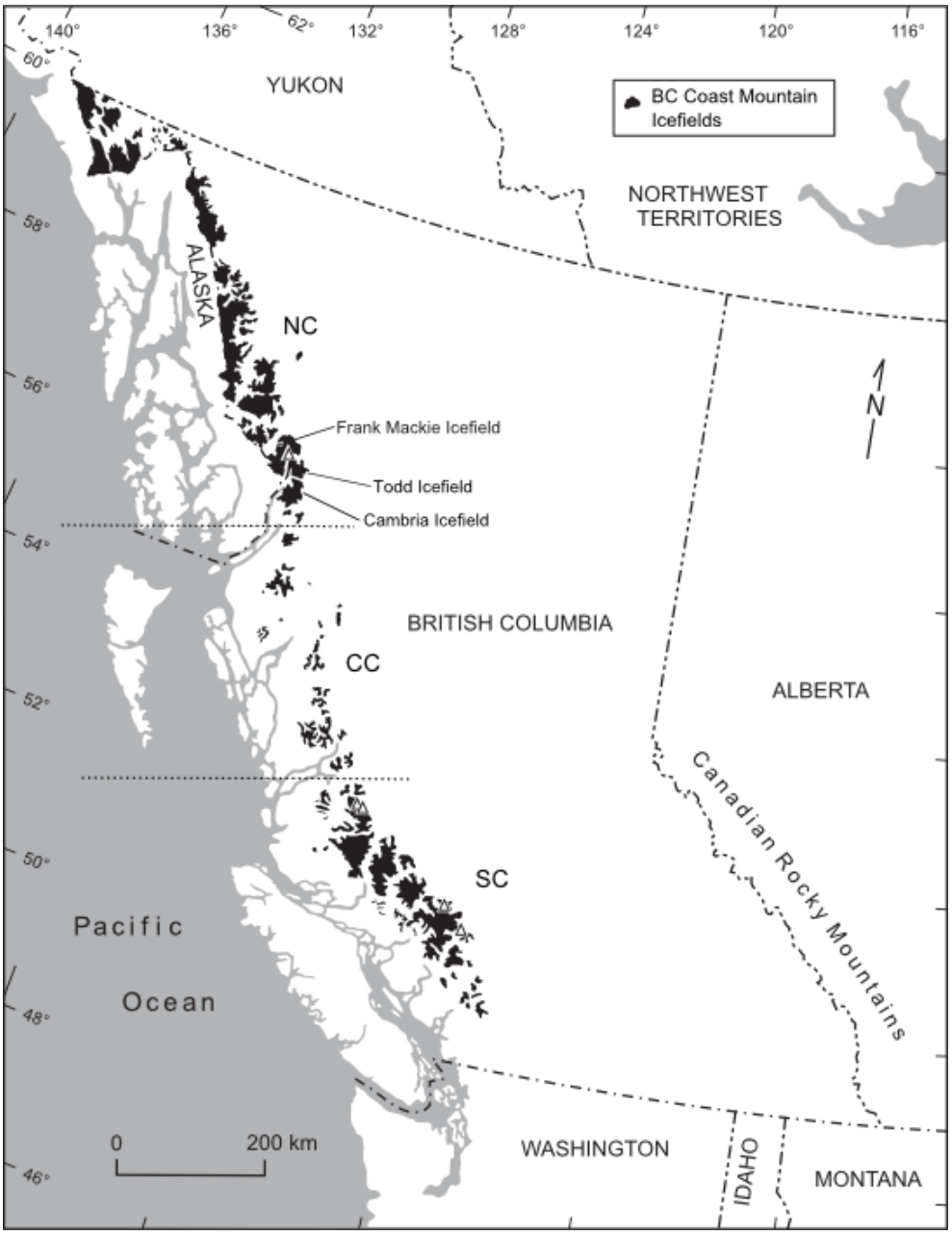

Figure 1.1: Map showing the locations of major glaciers and icefields of the northern (NC), central (CC) and southern (SC) British Columbia Coast Mountains.

1.1 Goal and Objectives

The purpose of the research presented in this thesis was to reconstruct the Holocene glacier history of the Bowser River Watershed. Specific objectives were to:

1. Determine periods of glacier advance and retreat by using principles of minimum and maximum limiting ages acquired by radiocarbon dating, dendrochronology and stratigraphic records.
2. Describe the behaviour of glaciers at the watershed scale by integrating newly collected data with previous findings.

1.2 Thesis Format

This thesis consists of eight chapters. Chapter 1 introduces the thesis. Chapter 2 provides a background on late Quaternary glacier advances and the techniques used to date them. Chapter 3 introduces the study area and reviews the findings of previous research. Chapter 4 focuses on the dendroglaciological methods used in this study. Chapter 5 provides observations from the field sites, and radiocarbon and dendrochronological results. Chapter 6 presents interpretations of the field sites. Chapter 7 expands the discussion of periods of regional advances in the northern Coast Mountains. Chapter 8 summarizes the findings of the thesis and considers limitations and suggestions for future research. Supplementary data is included in the appendices.

Chapter 2: Literature Review

Glaciers worldwide have been in retreat since the end of the Little Ice Age (LIA) in the late 19th century (Mann, 2002). Accelerated retreat in the last few decades is attributed to anthropogenically-induced warming associated with the increased concentration of greenhouse gases in the atmosphere (Hegerl et al., 2007). In the northern BC Coast Mountains, glaciers have experienced accelerated retreat during the latter half of the 20th century and overall have demonstrated a strong negative mass balance (Schiefer et al., 2008). Understanding the causes and mechanisms that trigger glacier advance and retreat is necessary to place ongoing climate changes into a broader historical context. This chapter begins with a discussion of the climate forcing mechanisms that affect global and regional climates. This discussion is followed by a review of the Quaternary glacial history of northwestern North America[1]. The chapter concludes with an overview of the primary techniques used in the reconstruction Quaternary environments.

2.1 Climate Forcing Mechanisms

Multiple mechanisms have been suggested for triggering abrupt climate change. On longer time scales, the Earth has experienced Milankovitch cycles, which are based on the Earth's eccentricity as it orbits the Sun, its axial obliquity and the precession of the equinoxes. The three cycles have different periods, which affect

1 Dates presented in this literature review are written as they appear in the publications. It is assumed that dates are provided in calendar years, unless stated otherwise with ^{14}C.

the amount of solar radiation received at different places on Earth's surface (Wright, 1984). During periods when eccentricity, obliquity and precession align in their low solar radiation states, the solar input can be effectively low enough to alter circulation patterns of the atmosphere and ocean (Adams et al., 1999).

During the last glacial period, from 80 to 18 ka, the Earth experienced abrupt changes in its climate system as recorded by changes in oxygen-16 and oxygen-18 isotopes in Greenland ice cores (Schmidt and Hertzberg, 2011). Twenty-five millennial-scale oscillations representing changes from stadial and interstadial conditions are known. These oscillations are referred to as the Dansgaard-Oescherger cycles (D-O cycles) (Schmidt and Hertzberg, 2011). Shifts to interstadial conditions occurred over periods of several decades. By contrast the return to stadial conditions was much more gradual. This difference is reflected in the 'saw-tooth' appearance of global oxygen-isotope records (Schmidt and Hertzberg, 2011).

The main hypothesis put forward to explain the D-O cycles is the 'Salt Oscillator Hypothesis', which is based on salinity levels of the Atlantic Ocean's Conveyor System (Broeker et al., 1990). A decrease in salinity is controlled by fresh meltwater input and salt export. During periods when the salinity and thus density of the deep waters are low, the conveyor begins to slow down or even stop as north Atlantic waters no longer circulate to the southern ocean (Broeker et al., 1990). This change causes a shift to stadial conditions, allowing ice sheets to grow. The subsequent reduction of meltwater from glacier growth and reduced salt export from the stopped conveyor ultimately causes the conveyor to recommence and continue the cycle (Broeker et al., 1990).

There have also been proposed hypotheses for climate forcing mechanisms operating on shorter time scales, such as the Holocene Epoch. These mechanisms include changes in atmospheric circulation (Gavin et al., 2011), disruption of thermohaline circulation (Gavin et al., 2011), volcanic forcing (Wanner et al., 2008), variation in solar irradiance (Denton and Karlén, 1973), and shifts in the position of the polar jet stream. These mechanisms are often discussed in the context of singular climate events such as a period of glacier advance or retreat.

Over shorter intervals the Pacific Decadal Oscillation (PDO) and El Nino Southern Oscillation (ENSO) are important when reconstructing past climate fluctuations (Gavin et al., 2011). Many dendrochronology records demonstrate repetitive patterns influenced by both PDO and ENSO (Larocque and Smith, 2005; Johnson and Smith, 2012). These oscillations are controlled by sea surface temperature and circulation. PDO and ENSO have warmer and colder phases, and must be understood and identified for proper interpretation of climate and climate proxy data sets.

Cyclic phases of ENSO and PDO have varied spatially and temporally over the Holocene. There is evidence that they were suppressed during the mid-Holocene, while PDO became more positive and variable during the late Holocene (Barron and Anderson, 2011). More recently, decoupling between PDO and winter mass balance is visible in the instrumental records and summer mass balance has become a much better predictor of net mass balance. The recent warming trend of the last century is hypothesized to be the reason for this decoupling (Malcomb and Wiles, 2013).

2.2 Quaternary Glaciations

The Quaternary Period is subdivided into the Pleistocene Epoch from 2.58 Ma to 11.7 ka cal. yr BP, and the Holocene Epoch from 11.7 ka cal. yr BP to present. Another subdivision of the Quaternary Period, termed the Anthropocene has been gaining recognition in recent years (Steffen et al., 2007; Zalasiewcz al., 2010). This proposed epoch, which began at approximately 1800 ad., is based on the impact of human activities that are modifying the biosphere at a much faster rate than ever before (Crutzen, 2006).

The present interglacial period is climatically benign compared to the last ice age, although we now are acquiring a better understanding of the multiple glacier advances and retreats have occurred during the last 11.7 ka years. Climate during the Holocene has not remained stable (Rousse et al., 2006), which has triggered fluctuations in glacier mass balance. The Holocene Epoch can be divided into three periods: early, mid- and late (Figure 2.1).

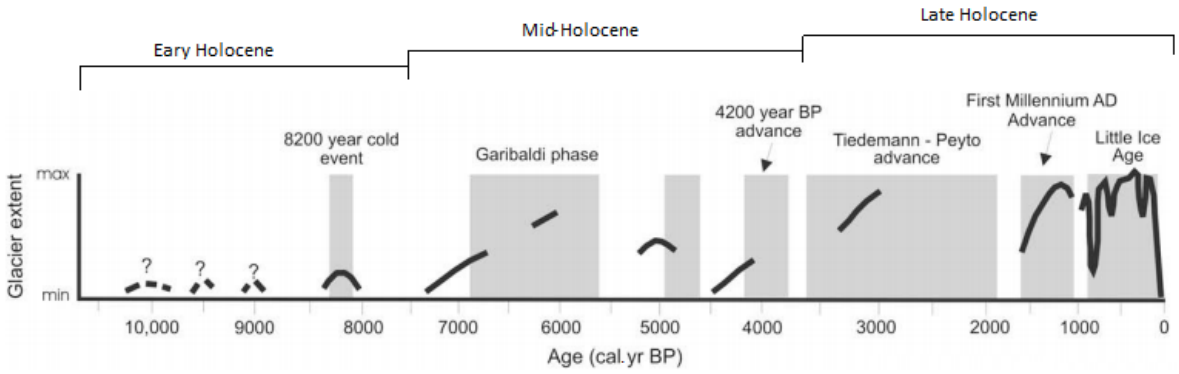

Figure 2.1: Division of the Holocene epoch into early, mid and late Holocene periods. Illustrated are the major periods of glacier expansion and relative extent of glaciers in the BC Coast Mountains. Modified from Clague et al. (2009).

2.2.2 Nomenclature of Holocene Glacier Events

Glacier advances are often discussed as singular events followed by periods of negative mass balance and retreat. This study suggests a more complex glacier history during the Holocene, where during the mid- and late Holocene glaciers have fluctuated rapidly within known 'advances' such as in the LIA (Figure 2.1). In other instances, named glacier events are so close in time that it is unclear why they should be considered separate advances, illustrated by the 4.2ka and Early Tiedemann advances. The Early and Late Tiedemann events, by contrast, are separated by a much longer period of more than 500 years. It can be suggested that current nomenclature for glacier advances is not appropriate and does not reflect our more developed chronology of glacier events. Clague et al. (2009) discusses this issue and suggests limiting the term 'advance' to a singular, well defined and dated event, whereas the term 'phase' should be used to define a series of advances separated by small periods of retreat.

To facilitate comparison between this study and others, this report will continue to utilize current nomenclature for glacier advances. With continued increase in the resolution of Holocene events we may find that glacier history is too complex to employ current nomenclature.

2.2.1 Late Pleistocene (16,500-11,500 cal. yr BP)

Large ice sheets covered much of North America during the Pleistocene. The Cordilleran Ice Sheet (CIS) covered southern Alaska, southern and central Yukon and nearly all of BC (Figure 2.2). The ice sheet achieved its greatest maximum extent

at approximately 16.5 ka cal. yr BP. The next 5000 years have been described as “a time of flickering climate” due to the rapid transitions between glacial and interglacial states (Menounos et al., 2009).

Four stages have been proposed to describe the deglaciation of the CIS: i) active ice phase; ii) transitional upland phase; iii) stagnant ice phase; and, iv) dead ice phase (Fulton, 1991). Deglaciation was controlled primarily by topographically controlled downwasting in low-lying areas of the BC Interior Plateau (Fulton, 1991). Glacial expansion during the Younger Dryas cold period followed separation of the CIS and the Laurentide Ice Sheet (LIS), and was the last of the D-O cycles (Broecker et al., 1990).

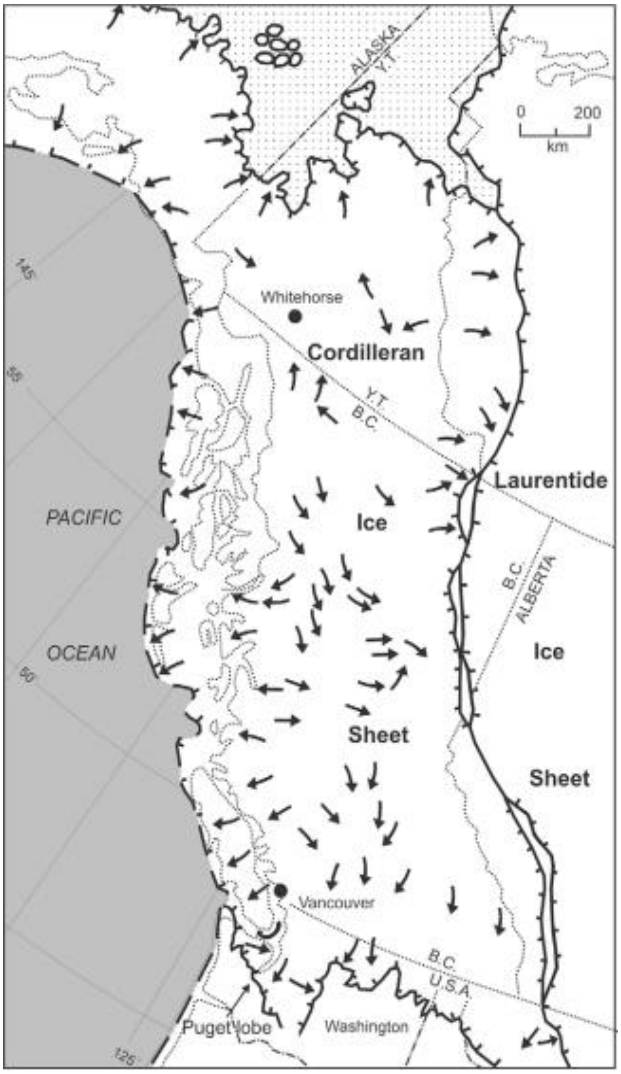

Figure 2.2: Extent of the Cordilleran Ice Sheet during the Pleistocene epoch (from Clague et al., 2000, modified from Flint, 1971).

The Finlay Advance is recorded by moraines with a minimum age of 10.5 ka cal. yr BP (Lakeman et al., 2008). The moraines, located in the northern Rocky Mountains of BC, are sharp-crested and their size is attributed to the abundance of accessible sediment during latest Pleistocene deglaciation (Lakeman et al., 2008). The glaciers that built these moraines were 5-10 times greater in area than those during the LIA (Menounos et al., 2009). Limiting ages of the Finlay Advance come

from radiocarbon ages on unidentified terrestrial macrofossils in sediment cores collected from six lakes in the southern Cassiar Mountains (Lakeman et al., 2008). Minimum limiting ages of 11-10.75 ka cal. yr BP for the abandonment of moraines were obtained on wood in a core from Sandwich Lake, located where lateral meltwater channels crosscut Finlay moraines (Lakeman et al., 2008).

2.2.3 Early Holocene (11,500-7500 cal. yr BP)

The Holocene Thermal Maximum (HTM) or Hypsithermal, which was a time when temperatures were warmer than today, spanned much of the early Holocene (Terasmae, 1961). Onset of the HTM began with the retreat of the LIS coupled with a higher solar insolation maximum (Fritz et al., 2012). In the northern Yukon, pollen and plant macrofossils (*Picea* and *Populus*) have been found 75-100 km north of their present-day limits (Fritz et al., 2012). Vegetation spread in the northern Yukon was initially limited by the dry conditions; however, climate began to shift to more moist conditions due to a rising glacio-eustatic sea level and the reduction in sea ice coverage (Fritz et al. 2012).

Lacustrine records indicate that the climate in southwestern Yukon and interior Alaska was predominantly warm and dry during the early Holocene (Gavin et al., 2011). Pollen records from this region substantiate this finding (Bunbury and Gajewski, 2009) and demonstrate that vegetation did not adapt well to the xeric conditions in Alaska during the HTC (Fritz et al., 2012). Farther south, in the Iskut region of BC, pollen records indicate enhanced vegetation and forest productivity (Spooner et al., 2002). It is hypothesized that the large variations in pollen abundances and organic matter in Iskut region samples during the early and middle

Holocene samples are due to a greater frequency of fires than today (Spooner et al., 2002).

While climate was, on average, warmer and drier than today, at least one early Holocene glacier advances is recorded in northern BC. This cooling event is referred to as the 8.2 ka event (Alley and Agustsdottir, 2005). Strong evidence for abrupt cooling at ~8000-8400 yr BP is recorded by a sharp decrease in methane and $\delta^{18}O$ levels in Greenland ice cores (Alley et al., 1997). It is estimated that the climate shift during this event was approximately half the magnitude as that of the Younger Dryas (Alley et al., 1997) and was similarly triggered by catastrophic release of freshwater into the Atlantic (Cronin et al., 2007). Synchronous regional correlatives signify that the event occurred at a hemispheric scale (Kobashi et al., 2007). Evidence for the 8.2 ka event in the Coast Mountains is limited to lake sediments and detrital wood found in a glacier forefield in Garibaldi Park (Menounos et al., 2004).

2.2.4 Mid-Holocene (7500-3500 cal. yr BP)

The Neoglacial period is the growth and expansion of alpine glaciers during the mid-Holocene which followed significant retreat during the Hypsithermal Interval (Porter and Denton, 1967). The shift from the warm, dry climate of the Hypsithermal Interval to the cooler, wetter climate of the mid-Holocene is thought due to stabilization of sea level during an interval of negligible contribution of melt water and maximum variation in solar insolation (Debret et al., 2009).

The durations of the Neoglacial and Hypsithermal intervals differ regionally. The first glacial advance during the Neoglacial interval was the Garibaldi Phase,

which lasted over a millennium from 7 to 6 ka cal. yr BP. There is no evidence for the Garibaldi Phase in the Canadian Rocky Mountains, thus the term is generally not applied there (Osborn et al., 2007). An unnamed, late Garibaldi Phase glacier expansion is based on findings at Canoe and Tchaikazan glaciers where radiocarbon-dated detrital wood fragments record a time when glaciers advanced into forests at 5450–5050 and 5590–5080 cal. yr BP respectively (Harvey et al., 2012).

Evidence for glacier advance at 4.2 ka cal. yr BP includes radiocarbon ages on in-situ stumps in southern and central BC (Menounos et al., 2008). An increase in clastic sedimentation and associated low loss-on-ignition values have been found in lake cores dating to the period of 4.2-3.8 ka (Menounos et al., 2008). In the northern Coast Mountains, the preservation of multiple caribou antlers, of which one provided a date of 3.8 ka yr BP, was interpreted by Ryder (1987) to indicate a cold and wet climate since the end of the mid-Holocene to present.

2.2.5 Late Holocene (3500 cal. yr BP - present)

Three major periods of regional glacier advances during the late Holocene are recognized: The Tiedemann Advance at 3.3-2.2 ka (Ryder and Thomson, 1986), which occurred synchronously with the Peyto Advance in the Canadian Rocky Mountains (Osborn et al. 2012); the First Millennium AD (FMA) advance from 1.6-1.4ka (Reyes et al., 2006); and the LIA from 900 to 100 cal yr BP. The use of the term 'advance' has been criticized, particularly with reference to the Garibaldi phase, Tiedemann-Peyto Advance and the LIA, as the term may not adequately capture the complexity of glacial activity during that period (Clague et al., 2009). This issue is

discussed by Koehler and Smith (2011), who documented an expansion of glaciers at 2.42 ka in the southern Coast Mountain glaciers that they refer to as the Manatee Advance. This episode is differentiated from Tiedemann-age advances by the preceding extensive loss of glacier mass that had occurred following the Tiedemann Advance at 3.70 ka (Koehler and Smith, 2011).

Radiocarbon ages and tree ring, sediment cores and lichenometry data indicate the onset of the Neoglacial period occurring around 3-4 ka in Alaska (Barclay et al., 2009). A core from Waskey Lake pinpoints the onset to approximately 3.2 ka. Magnetic susceptibility decreases at this level in the core and the ratio of kaolinite:quartz increases, coincident with the onset of a glacier advance (Barclay et al., 2009). Grain size and organic matter content decrease (Barclay et al., 2009) as fluvial inputs decreased with the onset of glaciation. Bear River Glacier in northern BC also advanced during this period at 3.3-3.7 ka at the same time (Jackson et al., 2008; Osborn et al., 2013).

Evidence of the FMA in Alaska comes from cross-dated logs that were killed by advancing glaciers (Wiles et al., 2008) and from lichenometry (McKay and Kaufman, 2009). A period of moraine construction spans much of the First Millennium AD. Three advances occurred in the Kenai, Chugach and Coast Mountains during the LIA. The largest advances of the Holocene Epoch in Alaska occurred during the LIA (Barclay et al., 2009).

Records of late Holocene advances in northwestern North America are more plentiful than those of the earlier Holocene. It is possible that evidence of early advances has been destroyed by the later advances, particularly those of the LIA

(Hart et al., 2010) (Figure 2.1). Evidence for post-Pleistocene glacial maxima during the LIA advances is found in the northern Coast Mountains (Ryder, 1986), southern Coast Mountains (Allen and Smith, 2007; Ryder and Thomson, 1986) and the Rocky Mountains (Luckman, 1995; Luckman, 2000). Glacier mass balance reconstructions for the LIA in BC demonstrate that glacier fluctuations were synchronous throughout Vancouver Island, the southern Coast Mountains and the Rocky Mountains (Malcomb and Wiles, 2013).

2.3 Dating Methods

A variety of relative and absolute dating techniques can be used to determine times of past climate events. The selection of techniques and methods depend on a combination of factors: what datable material is available at the field site, the expertise of the researcher, and time and cost constraints of the study. Common dating methods include stratigraphy, radiometric dating and dendrochronology. These are the primary methods that I used in this study.

The identification of sedimentary deposits is essential in reconstructing glacier history. The morphology, location, lithology and sedimentology of sediments provide clues about glacier dynamics. Sediments are deposited by aeolian, fluvial, glacial and mass wasting processes. Depositional landforms and their composition reflect the method of transport and the environment during the time the sediment was deposited.

Understanding the sequential relationship between surficial deposits and glacial and interglacial periods allows us to recognize order in stratigraphic sequences (Clague, 2000). Sedimentary sequences can differ depending on the local

landscape. During interglacial periods, plateaus tend to not experience large amounts of deposition or erosion in contrast to glacial periods when significant erosion occurs. Valleys are the dominant area of deposition during glaciations, while sediment tends to get relocated downstream to coastal regions and lakes in interglacial periods (Clague, 2000).

Although studies of deposits are useful, unconformities in sediment sequences can provide valuable information about glacier fluctuations. Unconformities are interruptions in a sedimentary sequence, caused by both glacial and non-glacial erosion. Non-glacial unconformities are caused by fluvial erosion and mass wasting. This recognition is critical when studying sediments in the field to reconstruct a history of physical processes (Clague, 2000).

While stratigraphy can provide relative ages of sedimentary layers, dating methods such as radiocarbon dating are necessary to provide absolute ages of deposition. Radiocarbon dating is based on the measurement of the carbon-14 (^{14}C) radioisotope in organic matter following death. Radiocarbon years are expressed in years before present (BP), where BP is set as 1950. Radiocarbon ages must be calibrated because the atmospheric concentration of ^{14}C has fluctuated over the course of Earth's history (Walker, 2005). The concentration of atmospheric ^{14}C is influenced by the carbon cycle, solar variability, and cosmic ray flux (Blaauw et al., 2004).

Dendrochronology is the science of dating tree rings. It is a high-resolution dating technique that provides yearly and seasonal chronologies. Because dendrochronology provides an exact calendar date, it has been essential in

calibrating radiocarbon ages (Speer, 2010). The patterns and spacing between rings can provide clues about past climate regimes, as well as insights into disturbances such as insect infestations, fires, landslides and avalanches. Dendrochronology studies have become more prominent in recent years, and chronologies have been built using evidence from numerous glaciers in the Coast Mountains (Wilson and Luckman, 2003;Tomkins et al., 2008; Harvey et al., 2012).

The science of dendrochronology includes the subfield of dendroglaciology, which uses tree rings to date the advance and retreat of glaciers. Chronologies from living and dead trees, as well as disturbances in ring patterns can be used (Hart et al., 2010). In-situ samples that have been killed by an advancing glacier can provide a date for the expansion of the ice margin (Harvey et al., 2012) and provide a maximum limiting age of the advance.

The abandonment of moraines provides a minimum limiting age for glacial retreat. These ages are based on stabilization of the moraines by vegetation. Consideration must be given to the time it takes for stabilization of the moraine to seedling germination, which is known as ecesis, (Clague et al., 2010). Research relying on dendroglaciological methods in the Coast Mountains include studies by Allen and Smith (2007) and Jackson et al., (2008).

It is useful to employ multi-proxy methods in paleoenvironmental studies, though issues can arise when trying to directly compare different datasets. An example is provided by Tompkins et al. (2008), who analyzed varves and tree ring chronologies from Mirror Lake, North West Territories. They compared the proxy records with meteorological data for the period of 1967-1990. The correlation was

high for the first decade, but only moderate for the second decade. However comparing varve thickness to tree ring width for the period of 1704-1996, revealed no statistical significance between the proxy records (Tomkins et al., 2008). A limitation in comparing proxies is that they respond to different mechanisms and sensitivities, resulting in records of different climate signals.

2.4 Summary

The growth and retreat of glaciers is influenced by a variety of climate forcing mechanisms. On longer time scales Milankovitch cycles have paced glacier cycling. These cycles resulted in large ice sheets covering the majority of Canada at times during the Pleistocene Epoch. The Holocene Epoch was relatively benign by comparison. The early Holocene experienced a warmer climate than today, and the Neoglacial period, which began in the middle Holocene, was characterized by an expansion of glaciers. The mid- and late Holocene is punctuated by several glacier advances. Techniques, such as radiocarbon dating and dendrochronology, combined with stratigraphic records, allow researchers to date and interpret past glacier activity.

Chapter 3: Study Area

3.1 Location

The Bowser River Watershed (BRW) is located in the Boundary Ranges, the largest range of BC's northern Coast Mountains. The watershed encompasses the area from 56°09' to 56°29' N and 129°23' to 130°16' W and is part of the Cassiar Land District. The Frank Mackie and Todd icefields feed many of the major valley glaciers. Frank Mackie Icefield feeds Berendon, Knipple, Charlie, Canoe and Frank Mackie glaciers, and Todd Icefield feeds Todd, Sage and Bug glaciers (Figure 3.1). There are also a number of small unnamed cirque glaciers within the watershed. Glacier melt water flows into the Bowser River and its tributaries, which drain into Bowser Lake.

3.2 Access

The nearest communities to the study area are Stewart BC (55°56′09″N 129°59′27″W) and Hyder, Alaska (55°54′51″N, 130°1′27.7″W), which are located 30 km southwest of the southernmost portion of the watershed. The BRW is accessible by two roads. The northern access road, which is connected to Cassiar Highway, was in a state of redevelopment as of June 2013. The southern access road extends north from Stewart and Hyder and is used for mineral exploration and tourist access to Salmon and nearby glaciers.

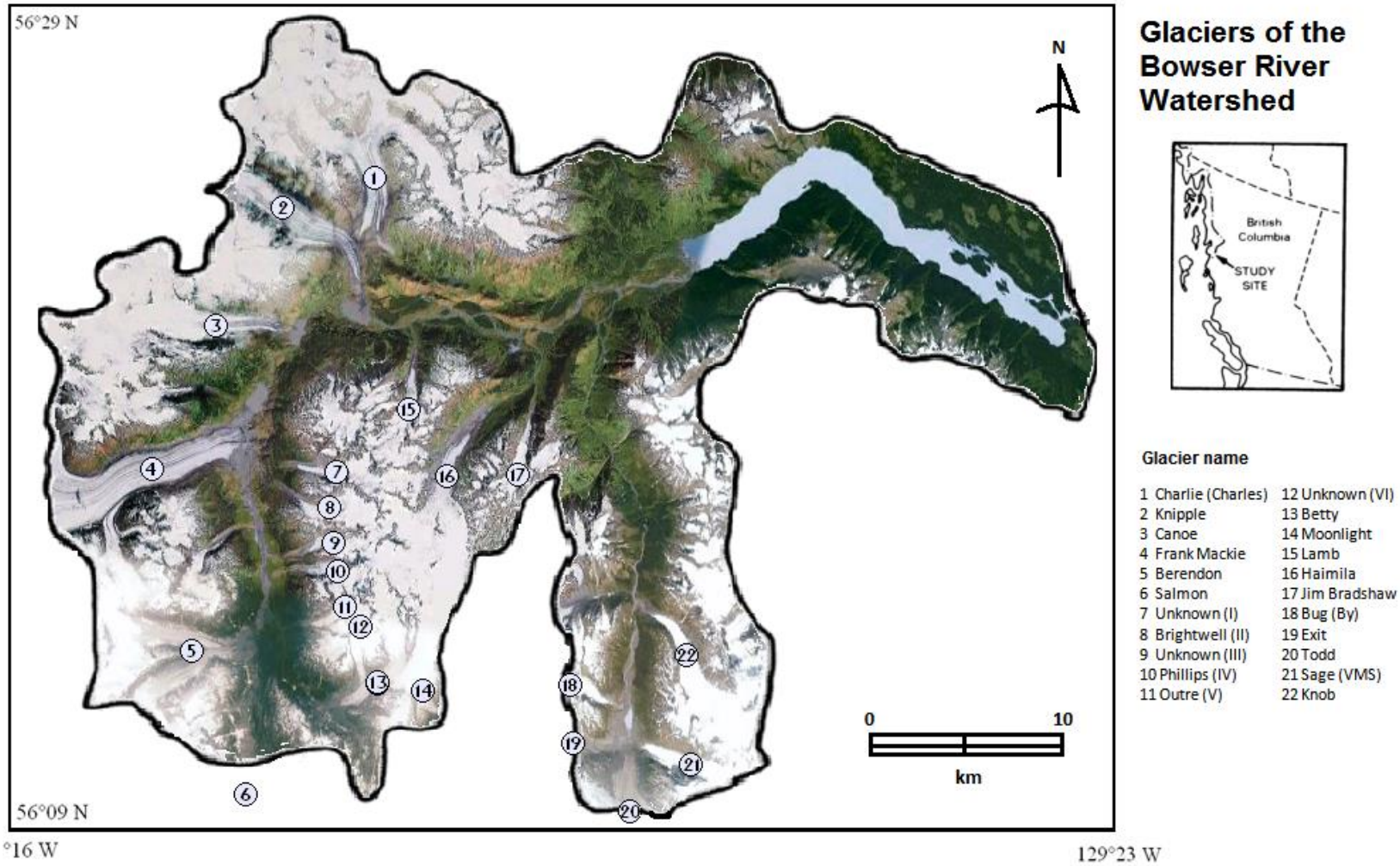

Figure 3.1: Location of glaciers in the Bowser River Watershed referred to in the text. Image from Google Earth (2013), watershed outline and inset map from Gilbert et al. (1997). Alternative names for glaciers are listed in brackets.

3.3 Geology

The western region of the BRW is underlain by the Stewart complex, which comprises volcanic rocks of Upper Triassic to Late Jurassic age, and the Bowser Lake Group consisting of Middle Jurassic sedimentary rocks (Aldrick, 1988). The region is important to the mining industry, hosting over 800 mineral occurrences (Metcalfe, 2013). Placer mining was the primary mineral exploration method from the early 1900s until the 1930s, after which lode copper-molybdenum and silver-gold deposits were discovered, although most claims remained unstaked until the 1960s (Hassan et al., 2012).

3.4 Ecology and Climate

The BRW is located within the Boundary Range Ecoregion and Southern Boundary Ranges Ecosection (BC Ministry of Environment, 2013). The landscape is dominated by a large alpine zone with numerous ice fields, glaciers and barren rock. Forests on lower valley slopes are dominated by subalpine fir and mountain hemlock, and valley bottom forest consists of western hemlock and Sitka spruce.

The BRW is characterized by a cold and wet climate resulting from moist Pacific air interacting with cold Arctic air masses. The nearest climate stations to the BRW are located at Stewart Airport (55°56'N, 129°59'W) and Todagin Ranch (57°36'N, 130°04'W) (Environment Canada, 2014). The two stations have very different climate regimes – the former has a maritime climate and the latter a more continental climate (Table 3.1). Annual air temperature at Stewart averages 6.1°C, ranging from an average of -5.5°C in January to 19.9°C in July. Approximately 30% of

precipitation at Stewart falls as snow. At Todagin Ranch, average air temperature is just below zero and average annual precipitation is 419mm.

Table 3.1: Climate normals for Stewart Airport and Todagin Ranch.

Station	Avg. daily temp. (^{0}C)	Max. daily temp. (^{0}C)	Min. daily temp. (^{0}C)	Total yearly precip. (mm)	Total precip. as snow (mm)
Stewart A[a] (7 m asl)	6.1	9.9	-4.3	1867	570
Todagin Ranch[b] (899 m asl)	-0.3	6.0	-6.5	419	161

[a](1980-2010) [b](1970-2000), (Environment Canada, 2014).

3.5 Previous Research

Research and mining activities in the BRW were triggered in response to mineral exploration in the region during the late 19th century. Many of the glaciers in the watershed, such as Charlie, Knipple, Frank Mackie and Haimila are named after prospectors who surveyed the region. Here, I review findings of previous research at glaciers within the BRW, including research at Salmon Glacier due to its historical impact on drainage in the BRW.

3.5.1 Salmon Glacier

Salmon Glacier is located south of the BRW within the Salmon River watershed. The glacier flows eastward across the Salmon River valley floor, where it bifurcates and flows to the north and south by an opposing bedrock wall (Haumann, 1960). The northern lobe impounds and calves into Summit Lake, creating an ice dam that during the LIA routed meltwater northward over the watershed divide into the Bowser River valley (Mathews and Clague, 1993). Prior to the 1960s Summit Lake was relatively stable and regularly overflowed to the north. In 1961,

1965 and 1967 there were catastrophic outburst floods into the lower Salmon River valley resulting from the drainage of Summit Lake beneath Salmon Glacier (Mathews and Clague, 1993). With further glacier retreat and downwasting, Summit Lake no longer overflowed to the north and episodically drained beneath Salmon Glacier (Mathews and Clague, 1993; Clark and Holdsworth, 2003).

The Holocene history of Salmon Glacier is unknown, as there are no previous reports describing its dynamics prior to the LIA. At present, retreat at the southern terminus is considerably greater than at the northern terminus, with surface area changes from 1985-2010 measured at -0.23%/yr (Beedle, 2012).

3.5.2 Berendon Glacier

Berendon Glacier forms from the coalescence of north and south tributary arms that flow east into the Bowser River valley (Figure 3.2). The first LIA advance in this area began more than 500 years ago and peaked in the early 17th century (Clague et al., 2004). An earlier Neoglacial advance began about 2800–3000 cal. yr ago and may have lasted for hundreds of years. There is also evidence for an intervening advance of smaller magnitude around 1200–1300 cal. yr ago (Clague et al., 2004).

A number of studies were initiated in the 1960s in response to mining activity adjacent to the glacier. A tunnel had been built to transport ore beneath Berendon Glacier from the Leduc mine. The tunnel portal and ore concentrator were near the terminus of the glacier and considered to be at risk of being destroyed if the glacier were to advance (USGS, 2002). Kinematic models measuring mass balance were constructed to predict if and when a positive mass balance would pose a risk

to nearby installations (Untersteiner and Nye, 1968; Fisher and Jones, 1971). It was noted that Berendon Glacier was retreating at the time of the study in the early 1960s, although future climate remained uncertain (Untersteiner and Nye, 1968). A later study by Eyles and Rogerson (1977) noted that rapid basal melt of the glacier terminus was being caused by the discharge of warm waste water from the concentrator that had been in operation from 1970 to 1975. During this period, ice loss at the terminus was continuous rather than seasonal and contributed to the development and subsequent collapse of ice bridges and ice-walled canyons near the glacier terminus (Eyles and Rogerson, 1977).

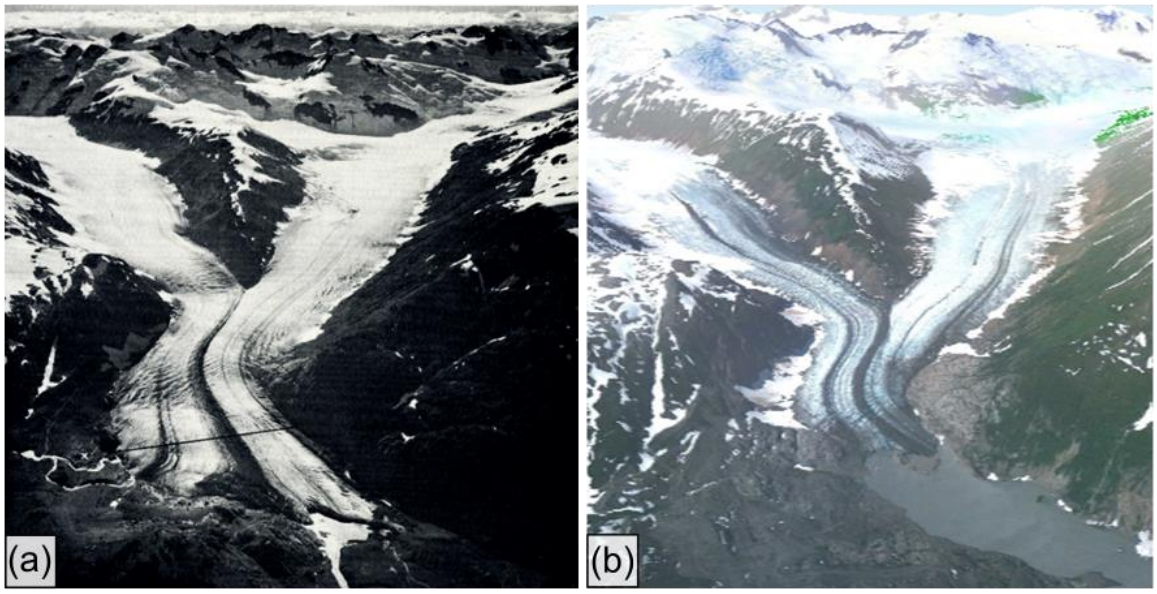

Figure 3.2: (a) Oblique air photo of Berendon Glacier in 1961 (Post, 1961). (b) 2009 Spot satellite (Google Earth, 2013).

3.5.3 Frank Mackie Glacier

Frank Mackie Glacier flows eastward toward Bowser River from the Frank Mackie Icefield (Figure 3.1). During the late Holocene, Frank Mackie Glacier advanced across the Bowser River valley to dam Bowser River and form Tide Lake.

The lake inundated the valley bottom between Frank Mackie and Berendon glaciers several times during the late Holocene (Haumann, 1960; Clague et al., 2004). At its maximum length of 8.5 km and width of 1.7 km, the lake impounded over 1 km^3 of water (Clague and Mathews, 1992).

The glacier dam failed several times during the Holocene due to thinning and retreat of Frank Mackie Glacier, producing outburst floods with effects that are recorded as far downstream as Bowser Lake (Clague and Mathews, 1992). Gilbert et al. (1997) noted that varves in the western basin of Bowser Lake contain strong acoustic reflectors of relatively coarse grained sediment beds. Although these reflectors could not be linked to specific events with certainty, they are suspected to be due to outburst floods or large storm events (Gilbert et al., 1997). Tide Lake last emptied around 1930 due to rapid incision of an end moraine that had impounded the lake (Clague and Mathews, 1992). Since then, it has not refilled due to continued retreat of Frank Mackie Glacier. Two small lakes presently lie adjacent to Frank Mackie Glacier: Toe Lake to its north and Head Lake to the south.

The drainage of Tide Lake in the early 1930s allowed Hanson (1932) to examine former lake bottom sediments and report that they consisted of over 5 m of varved clay (Grove, 1986). Clague and Mathewes (1996) undertook a multi-proxy study at the site that revealed four distinct phases of Tide Lake related to the advance and retreat of the snout of Frank Mackie Glacier. These phases include an undated advance older than 3000 BP, and advances at 2800, 1360 and 1000 yrs BP. The last phase of Tide Lake culminated during the 17th century and ended with draining early in the 20th century (Clague and Mathews, 1992).

3.5.4 Canoe Glacier

Canoe Glacier presently terminates adjacent to Tippy Lake in the Bowser River valley, 6 km down valley from Frank Mackie Glacier (Figure 3.3). Comparison of 1961 and 2003 imagery indicates that, while the glacier surface has been downwasting, there has been only a small amount of frontal retreat over that period (Figure 3.3). Harvey et al. (2012) report that Canoe Glacier was expanding into mature forests approximately 4570 and 3360±50 yrs BP (Figure 3.4)

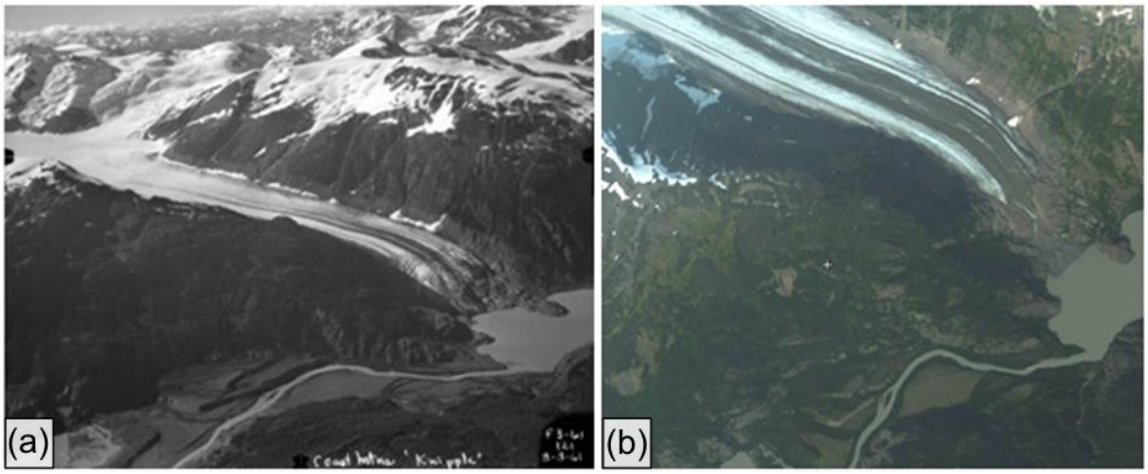

Figure 3.3: Comparison of extents of Canoe Glacier in 1961 (Post, 1961) and 2013 (Flash Earth, 2014).

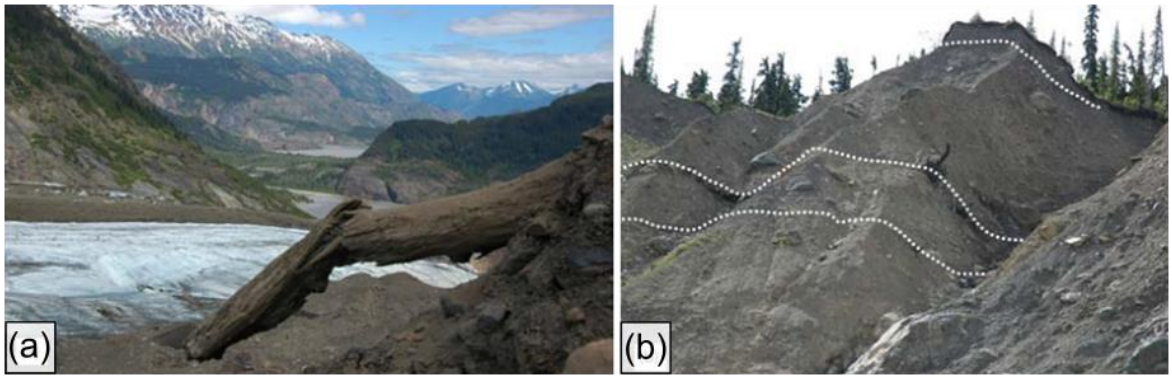

Figure 3.4: (a) Canoe Glacier with Tippy and Knipple lakes in the background. (b) Wood mats found in south lateral moraine of Canoe Glacier (from Harvey et al., 2012).

3.5.5 Todd Valley Glaciers

Todd Valley flows northward into the BRW, 20 km upstream from Bowser Lake (Figure 3.1). Dendroglaciological investigations at headwater glaciers close to the Todd Icefield indicate glacier expansion at 2300 and 690-1440 yrs BP, as well as three phases of LIA expansion beginning at 730 yrs BP (Jackson et al., 2008).

Chapter 4: Methods

Methods employed during this research can be divided up into field collection, data processing, analysis and interpretation. A flow chart of the general methods is shown below (Figure 4.1).

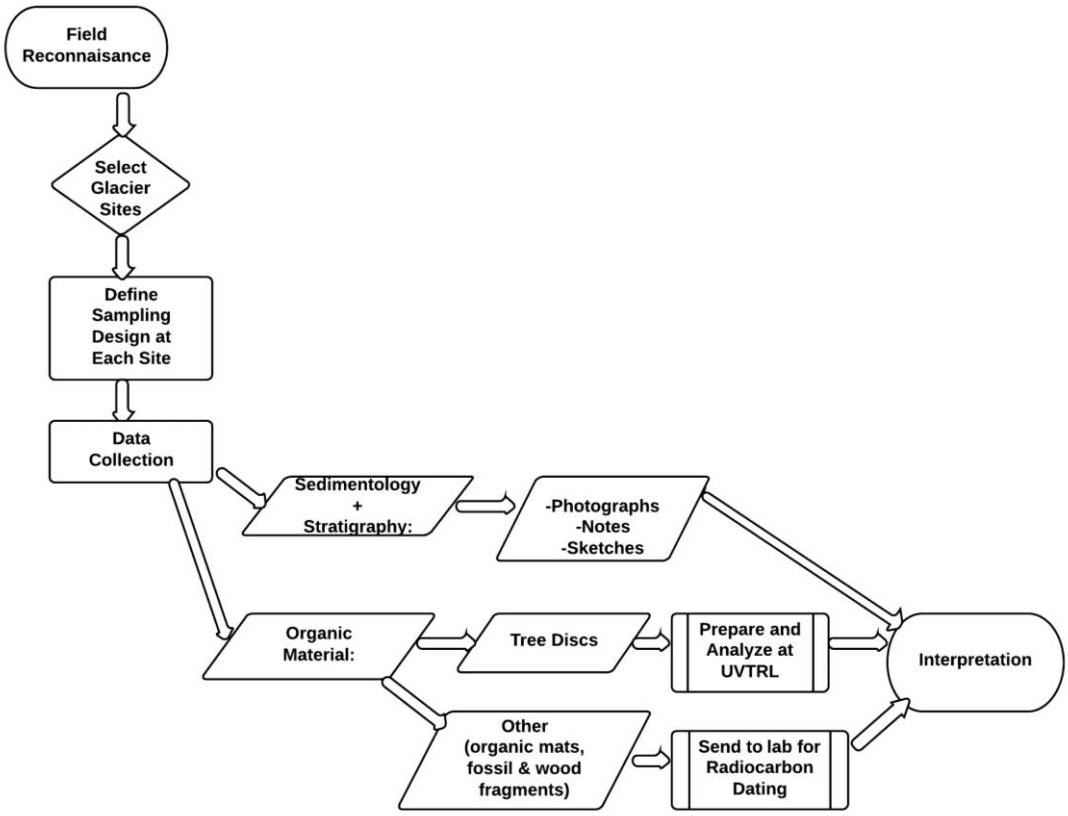

Figure 4.1: Methodological flow chart.

4.1 Reconnaissance and Sampling Design

Potential field sites were determined using satellite imagery and helicopter reconnaissance. Selection was based on accessibility, elevation below the tree line and presence of terminal and/or lateral moraines. Suitable sites needed to be accessible by truck, helicopter or hiking, with terrain safe enough to traverse. Reconnaissance investigations by truck and helicopter were used to access areas to search for woody debris.

4.2 Data Collection

Moraines and stratigraphic sections were surveyed and searched for organic material (tree logs and stumps, organic wood mats and fossils) deposited or disrupted by past glacial advances. Data recorded at each site included coordinates, location, elevation and descriptions of organic material, sediments and landforms. Sketches were made of stratigraphic sections and photographs were taken. Small bagged samples of organic mats and fossils were collected for later radiocarbon dating at Beta Analytic Laboratory. Tree logs and stumps were sawed into cross-section discs with a thickness of approximately 3-4 cm. The portion of the tree to be sawed was chosen to avoid breakage, rotten wood branch knots (Stokes and Smiley, 1968). The discs were wrapped with duct tape to prevent breakage during transport.

4.3 Data Processing and Analysis

The wood samples were examined at the University of Victoria Tree-Ring Laboratory. Wet samples were allowed to air dry before processing. Discs were

sanded to a fine polish using progressively finer sand paper on a belt sander (up to 600 grit paper) to reveal details in the tree ring boundaries and structure (Stokes and Smiley, 1968). Once polished, images of the discs were acquired using a 1200 dpi high resolution scanner. WinDENDRO (ver. 2012) software was used to measure ring widths to 0.01mm and to count the number of rings along two pathways on each disc from pith to perimeter.

Cross-dating matches patterns in tree ring widths in multiple specimens, allowing us to determine the range of years a tree was growing in (Eckstein and Pilcher, 1990). The International Tree Ring Database software program COFECHA was used to internally cross-date samples and then cross-date those to living chronologies (Grissino-Mayer, 2001). Internal cross-dating was necessary to locate and remove false rings and growth anomalies, which would otherwise affect the dating of the sample (Coulthard and Smith, 2013b). Once cross-dating was completed, the accuracy was checked using COFECHA through correlation statistics.

Correlation statistics were used to determine whether the subfossil samples collected in this research cross-dated to existing living and floating chronologies (Speer, 2010). The series correlation provides a measure of the strength of the climate signal present in all samples within a chronology (NOAA, 2014). Tree ring samples were cross-dated and statistically verified using 50 year segments lagged by 25 years with a critical correlation level (99%) of 0.40. The average mean sensitivity was also measured. The mean sensitivity is a "measure of the relative change in ring-width from one year to the next in a given series" (NOAA, 2014). Average mean sensitivity varies from 0.650 to 0.10, the former typical of drought-

sensitive trees, and the latter more complacent trees (NOAA, 2014). Ranges for average mean sensitivity are categorized as low (0.10-0.19), intermediate (0.20-0.29) and high (>0.30) (Grissino-Mayer, 2001).

Selected samples of perimeter wood were sent to Beta Analytic Inc. laboratory for standardized radiocarbon dating. Radiocarbon ages of the samples were calibrated using INTCAL09 calibration curve (Reimer et al., 2009) to account for fluctuations in the atmospheric $^{14}C/^{12}C$ ratio over time (Walker, 2005).

When a tree-ring chronology could not be cross-dated to living tree chronologies, the series was anchored using a radiocarbon dated sample from that chronology. The anchoring of the chronology was done using calibrated radiocarbon ages in lieu of conventional ages to facilitated comparison between radiocarbon anchored chronologies with living tree anchored chronologies, which are dated in calendar years. As the relationship between radiocarbon and calendar years is not linear, the accuracy of the calibration can be low, producing an age spanning several centuries. Plotting chronologies requires that a single date be assigned to the radiocarbon dated sample. The "wiggle-matching" dating technique is a commonly used method to accomplish this (Ramsey et al., 2001; Galimberti et al., 2004). Wiggle-matching assigns a calendar age to the sample by selecting the age(s) with the highest probability distribution produced by the calibrated age. To avoid subjectivity in assigning a calendar age to the chronology using wiggle matching, the calendar age was based on the mean 2α age range of the radiocarbon dated sample. Expansion on the method used for assigning calendar age to chronologies is further expanded and demonstrated in Appendix A1.

4.4 Interpretation

The principles of dendroglaciology (Table 4.1; Coulthard and Smith, 2013) were employed in this study to aid in interpreting the behaviour of BRW glaciers. Periods of glacier advance were discerned from the position and age of living and dead trees and disturbances found in the ring patterns. The radiocarbon ages assigned to floating chronologies provided approximate periods of glacier advance (Jackson et al., 2008).

Table 4.1: Principles of dendroglaciology (from Coulthard and Smith, 2013b).

Type of evidence	*Dating precision*	*Information provided*	*Potential limitations*
Glacially killed trees	Exact calendar date of tree death	In growth position: kill date indicates glacier position at a specific time Detrital wood provides limiting date for glacial event	Requires cross-dating to determine tree age or kill date Dating precision for an event depends on preservation of wood and loss of outer rings
Surface dating	10 years or greater	Age of the oldest tree provides minimum estimate for surface age	Ecesis interval can be difficult to estimate Assumption that the oldest tree has been sampled
Abrupt change in ring symmetry as a result of tilting	Exact calendar date of tilting event	Date of eccentric or abnormal growth indicates onset of event	Event may be severe enough to kill the tree; the floating chronology would require cross-dating
Ice-contact scars	Exact calendar date of damage or ice-contact event	Damage date indicates glacier position at a specific time	Scarred, living trees are often difficult to find Dead trees require cross-dating.

Interpretation of glacial events using the principles of dendrochronology requires an understanding of the geomorphic context in which samples were located. In-situ samples are able to provide a maximum-age of a glacier advance when dated, whereas detrital samples cannot as they have unknown provenance. The distinction between the in-situ and detrital is determined based on the sample condition, the presence of a paleosol, whether it is found on or within a paleosol or till and whether it cross-dates with other samples at its location. The samples were assigned to the following categories based on fulfilling one of the following characteristics:

In-Situ:

- Sheared stumps rooted in growth position.
- Boles and organic material found within a paleosol.
- Multiple boles in close proximity which are in standing position and are in clay substrate.

Detrital:

- Spilled or eroded wood found on the surface of moraines.
- Samples found in massive till and diamict units.

Detrital or in-situ:

- Boles and organic material found on or pressed into paleosols can be assigned either detrital or in-situ based on the following;
- Boles which cross-date with other radiocarbon dated sample(s) along the same laterally extensive paleosol or wood mat are assigned as in-situ. Multiple samples which cross-date together provide support for a single glacial event responsible for advancing into a standing forest.
- All other non-cross-dating boles and wood fragments found on or pressed into paleosols are considered as detrital, as it cannot be determined whether they were deposited from an upslope source (ie. mobilized during a landslide) or result from multiple glacier advances.

Chapter 5: Observation and Results

5.1 Introduction

Field investigations were completed at four glaciers in the BRW. Frank Mackie and Canoe glaciers were surveyed in July 2005 and 2006, respectively, and Charlie and Salmon glaciers were surveyed in July 2013 (Figure 3.1; Table 5.1). Summary results for individual field samples can be found in Appendix Table B.1.

Table 5.1: Locations of glacier field sites.

Glacier	Abbrev.	Site #	Site description	Coordinates (lat, long)
Charlie	KG	1	West lateral moraine	56°26'59" 123°58'52"
		2	East lateral moraine	56°28'00" 123°57'00"
		3	North side of Chas Lake	56°26'00" 123°57'46"
		4	South side of Chas Lake	56°25'47" 123°58'21"
Canoe	CAN	1	South lateral moraine	56°23'19" 130°4'8"
Frank	FM	1	Lower south moraine	56°19'31" 130°5'37"
Mackie		2	Upper south moraine	56°19'16" 130°5'43"
		3	Spill area below site 1	56°19'38" 130°5'30"
		4	MH and SAF stands, above site 2	56°19'19" 130°5'57"
		5	North lateral moraine	56°20'53" 130°05'38"
		6	Spill area below site 5	56°20'53" 130°05'38"
Salmon	SG	1	East side, proximal to moraine	56°11'33" 130°03'28"

5.2 Site Descriptions

5.2.1 Charlie Glacier

Knipple Glacier and its former tributary Charlie Glacier were likely named after Charles Knipple who prospected the Unuk-Stikine region from the early 1910s to the 1950s (The Ledge, 1912; Cremonese, 1986). In 2013 Knipple Glacier terminated 1.3 km north of Knipple Lake, while Charlie Glacier terminated on the east side of Mt. Knipple (Figure 5.1). Meltwater from eastern portion of Charlie Glacier collects in a small 1400 m long, proglacial lake, herein informally referred to as Chas Lake. Meltwater from Knipple Glacier and the west side of Charlie Glacier flows into Knipple Lake.

Comparison of 1961 and 2013 imagery demonstrates the extent of glacier retreat at this site (Figure 5.1a and 5.1b). Magnetometer maps of the termini demonstrate that both glaciers experienced minimal retreat from the 1960s to 1990 (Murton, 1990). As in 1961, Knipple Glacier still terminated at Knipple Lake in 1990, and Charlie Glacier abutted the east lateral moraine of Knipple Glacier. Since that time, Knipple Glacier has retreated approximately 1300 m, while Charlie Glacier has retreated 710-1100 m. This observation suggests that the majority of retreat at this site occurred within the past 20 years, with an average rate of frontal retreat of 56.5m/yr for Knipple Glacier and 30.9-47.8m/yr for Charlie Glacier.

When visited in 2013 the surface of Charlie Glacier supported numerous englacial streams and ponds, as well as several large bowl-like depressions with diameters tens of metres across. Many small (<1m) debris cones dotted the glacier

surface near the terminus. The glacier had three large medial moraines, which extended from the confluence of the two tributary glaciers at the north end.

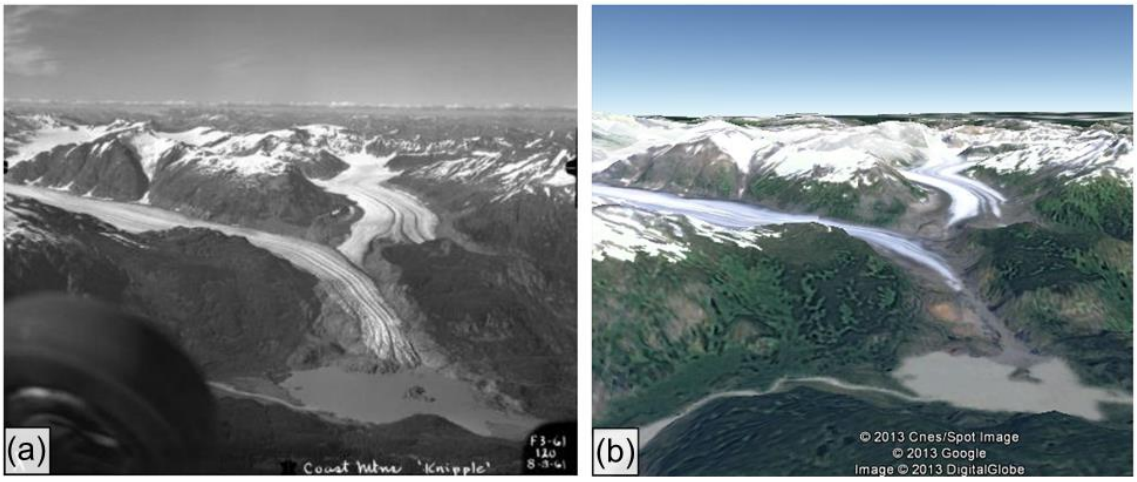

Figure 5.1: Comparison of (a) Knipple and (b) Charlie glaciers in 1961 (Austin Post, 1961) and 2013 (Google Earth, 2014).

Sample Sites

Samples were collected at four sites surrounding Charlie Glacier: Site 1- east-facing slopes; site 2- west-facing lateral moraine; site 3- north side of Chas Lake; and site 4- south side of Chas Lake (Figure 5.2). The glacier surface in July 2013 was 1045 m above sea level (asl) adjacent to site 1, and the level of Chas Lake was 843 m asl.

Figure 5.2: Locations of study sites at Charlie Glacier. (Modified from Google Earth, 2014).

Site 1- East-facing slopes: Site 1 is located on a steep east-facing lateral moraine slope between the terminus and exposed bedrock approximately 1.7 km north of the glacier terminus at 1050-1170 m asl (Figure 5.2). Boulders in the moraine are subrounded and elongated. The majority of the boulders are aligned north-south, parallel to the moraine, indicating possible ice streaming at the time of deposition.

A 1.3 m diameter bole (KG13-01) with a ^{14}C age of 3270 ± 30 yrs BP was found in growth position standing upright between the bedrock and till at 1080 m asl (Table 5.2). KG13-01 was interpreted to be in-situ from its upright growth

position along with additional small boles/sticks pressed into clay to silt sized sediment. Twenty-one additional detrital boles and wood fragments were collected nearby from the proximal surface of the eroding lateral moraine (KG13# 02-10, 14-25; Table 5.2).

Table 5.2: Radiocarbon ages from Charlie, Frank Mackie and Salmon glaciers.

Glacier	Sample ID	Description	Lat	Long	Elev. asl (m)	Conven-tional 14C age year BP	2 sigma Calibrated age range (BP)	Beta ID
Charlie	KG13-01	Standing, ice pressed into bedrock	56° 26' 59"	123° 58' 52"	1080	3270±30	3570-3440, 3420-3410	362278
	KG13-12	Buried soil horizon- wood mat	56° 26' 01"	123° 57' 49"	977	3260 ±30	3560-3440, 3440-3400	362279
	KG13-41	Spill from ice pressed logs	56° 25' 47"	123° 58' 21"	873	3230 ±30	3550-3540, 3480-3380	362283
	KG13-30	4m long bole in organic mat layer	56° 26' 01"	123° 57' 46"	1040	2620 ±30	2770-2730	362281
	KG13-31	Organic mat layer	56° 26' 01"	123° 57' 46"	1040	2460 ±30	2710-2630, 2620-2360	362282
	KG13-26	In situ stump buried in distal lat moraine	56° 28' 00"	123° 57' 51"	1228	470 ±30	540-500	362280
Frank Mackie	FM05-23	Gully, north moraine wall	56° 20' 53"	130° 05' 38"	757	2380 ± 40	2690-2660, 2480-2340	217006
	FM05-24	Gully, north moraine wall, on organic mat	56° 20' 53"	130° 05' 38"	755	2490 ± 40	2740-2370	217007
	FM05-03	Gully wall	56° 19' 31"	130° 05' 38"	700	1760 ± 40	1810-1560	242990
	FM05-04	Failure 'bowl', upright	56° 19' 31"	130° 05' 38"	705	870 ± 40	910-700	242991
	FM05-10	Hanging at top corner of gully wall/bowl	56° 19' 31"	130° 05' 38"	715	860 ± 40	910-850, 830-690	242992
	FM05-06	Failure 'bowl'	56° 19' 31"	130° 05' 38"	705	560 ± 50	660-510	242994
Salmon	SG13-01	Buried under sediment in pond, proximal to moraine	56° 11' 33"	130° 03' 28"	883	4950 ±30	5740-5600	362277

Site 2- West-facing lateral moraine: Site 2 is located along the east lateral moraine of Charlie Glacier at 1230 m asl (Figure 5.2). The moraine is well defined with a sharp crest, and extends 700 m down valley from the eastern glacier tributary (Figure 5.3a). The remains of an in-situ sheared, rooted stump (KG13-26) yielded a radiocarbon age of 470 ± 30 yrs BP. The sample was found partially buried in growth position on the distal side of the moraine at 1228 m asl (Figure 5.3b, Table 5.2). No additional samples were found at this site.

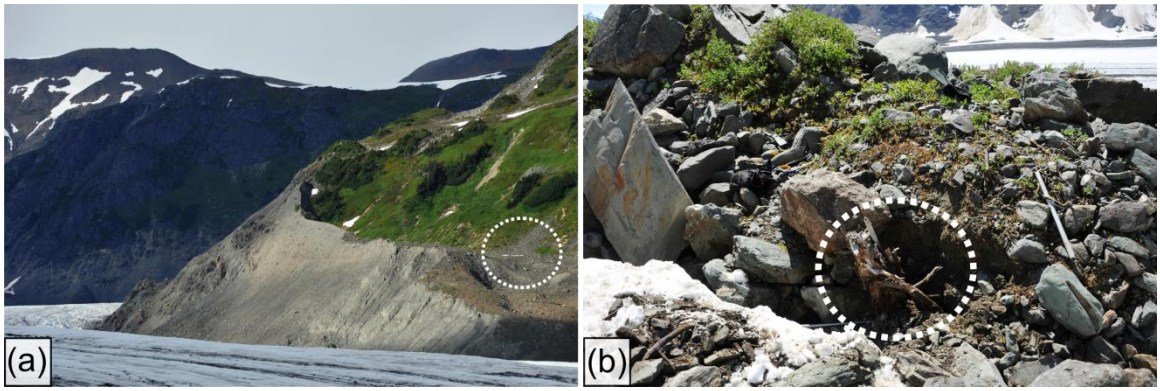

Figure 5.3: (a) East lateral moraine at Charlie Glacier (site 2). (b) In-situ stump on distal side of moraine (sample KG13-26).

Site 3 - North side of Chas Lake: Site 3 is located on a steep southwest-facing lateral moraine along the north side of Chas Lake (Figure 5.4a). Two laterally contiguous wood mats were discovered along the sides of gullies incised into the proximal face of the moraine (Figure 5.4b).

The upper wood mat in the eastern gully at 1040 m asl consists of woody detritus directly overlying an undisturbed buried soil. The soil consists of an Ah or O horizon with visible subalpine fir needles and an underlying orange-stained B horizon. Two in-situ samples were collected and radiocarbon dated: a small bole

(KG13-31) with a C^{14} age of 2460 ± 30 yrs BP that was pressed into the buried organic horizon; a 4 m long bole (KG13-30) with a C^{14} age of 2620 ± 30 yrs BP that extended outward from till 1 m above the buried surface.

A lower wood mat was located in the western gully at 977 m asl (Figure 5.4a). At this site a small wood fragment (KG13-12) with a C^{14} age of 3260 ± 30 yrs BP was found pressed into a buried podzolic soil horizon with distinct Ae, B and C horizons (Figure 5.4b). From its location over a paleosol, KG13-12 is interpreted to be in-situ. This interpretation is further supported by the number of radiocarbon and cross-dated samples which were similar in age. A large bole (KG13-29) of unknown length was found roughly at the same elevation in the eastern gully as the lower wood mat. The bole lay perpendicular to the gully, however it was unknown whether this sample can be considered in-situ as there was no evidence of a paleosol below. Fourteen addition surficial detrital wood samples were collected at site 3 on top of colluvium (Table 5.2) (KG13# 11, 13, 27, 28, 32-40).

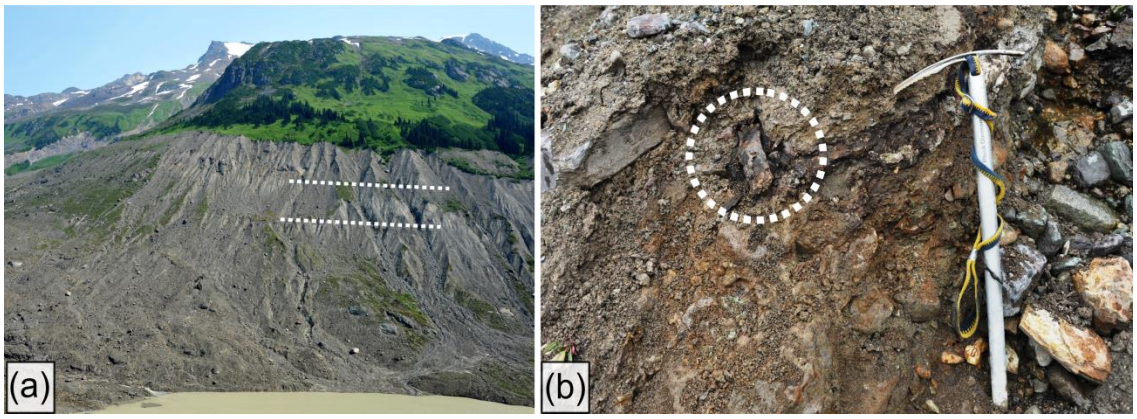

Figure 5.4: (a) Southwest-facing slope along the north side of Chas Lake (site 3). Dashed lines delineate organic mat layers. (b) Detrital wood found in lower organic layer above paleosol (sample KG13-12).

Site 4 - South side of Chas Lake: Site 4 is located along the west side of Chas Lake in an area of polished and grooved bedrock (Figure 5.5a). The remains of numerous detrital wood fragments and large boles are pressed into a cavity in the exposed bedrock at ~883 m asl (Figure 5.5b). Although the site was inaccessible, weathered remains of several large boles had fallen along the slope below. Perimeter wood from a large bole at 873 m asl (KG13-41) yielded a C^{14} age of 3230 ± 30 yrs BP.

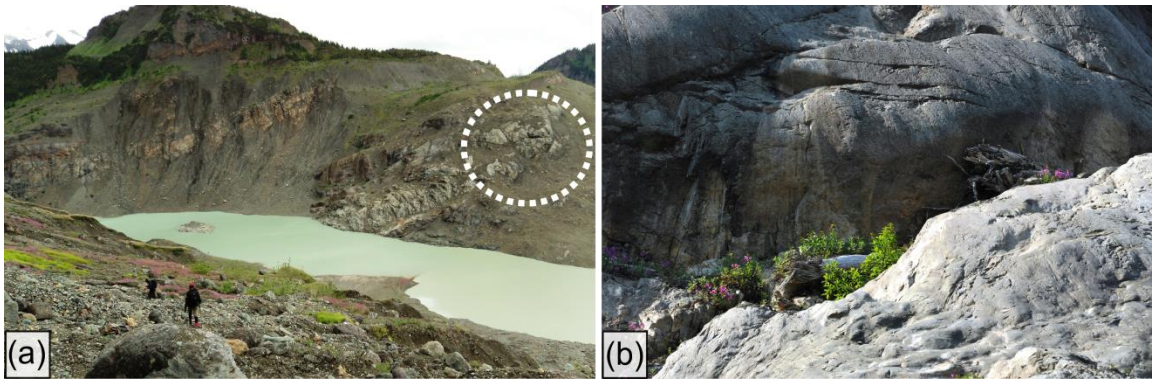

Figure 5.5: (a) View of bedrock outcrop on northeast-facing side of Chas Lake; site 4 circled. (b) Detrital wood in bedrock crevasse at Charlie Glacier (site 4).

5.2.2 Canoe Glacier

The southern lateral moraine of Canoe Glacier was surveyed in July 2006 (Figure 5.6a). Three wood mat horizons were found in the moraine (Figures 3.4b 5.6b). The two lower wood mats were 3.5 m apart at an elevation of approximately 747 and 750 m asl. The uppermost horizon at approximately 755 m asl was inaccessible. Two in-situ boles were retrieved from the second horizon (Can06#01, 02) and two from the third horizon (Can06#03, 11). In addition, 14 surface detrital wood samples were collected (Can06# 04-10, 12-17). Samples Can06-01 and

Can06-03 provided radiocarbon ages of 3720–3470 and 5450–5050 cal. yr BP respectively (Harvey et al., 2012), and were used in this thesis for crossdating.

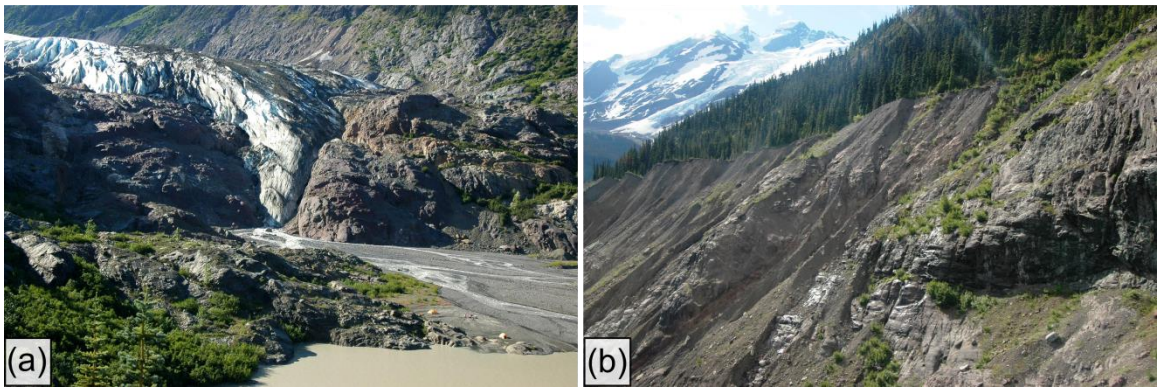

Figure 5.6: (a) Terminus of Canoe Glacier with Tippy Lake in foreground. (b) South lateral moraine.

5.2.3 Frank Mackie Glacier

Frank Mackie Glacier was surveyed in July 2005. Subfossil wood samples were collected from sites 1, 2, 3, 5 and 6 (Figure 5.7). Increment cores were collected from living mountain hemlock and subalpine fir trees at site 4 south of the glacier on an open rocky slope above the trimline. The living tree cores were taken to build a living chronology (UVTRL, *unpublished*). Cores of the mountain hemlock trees revealed ages of 200-300 years old, with all tree cores showing evidence of rot. A living tree chronology was built from trees from site 4, however detrital samples from Frank Mackie Glacier would not cross date to it, therefore the chronology was not used in this thesis.

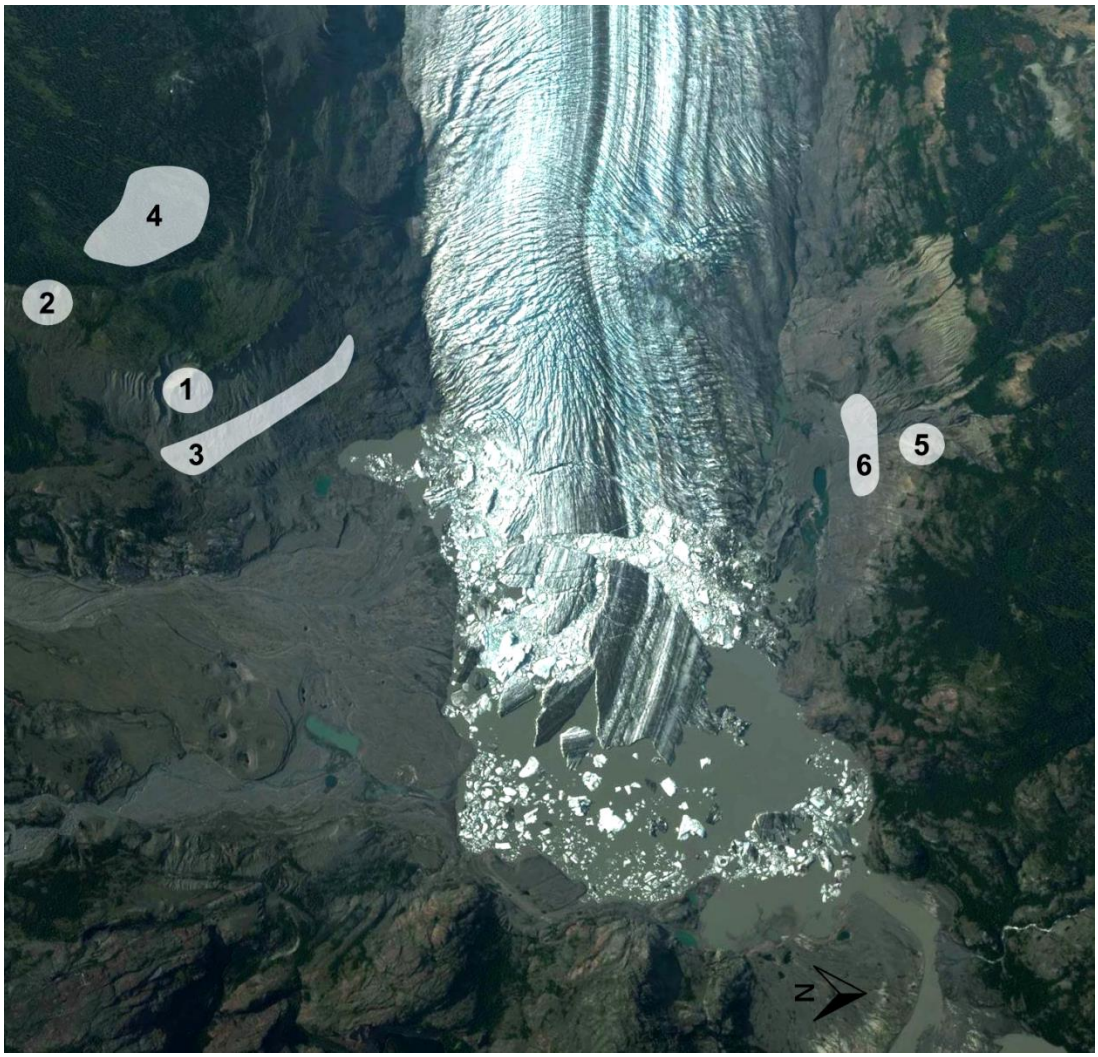

Figure 5.7: Locations of study sites at Frank Mackie Glacier (Modified from Flash Earth, 2009).

The glacier was inspected by helicopter in July 2013 for consideration of further field work. However, it was heavily crevassed at that time, and large icebergs had calved off the terminus, making it unsafe for glacier exploration (Figures 5.8a and 5.8b). The terminus of Frank Mackie Glacier underwent significant calving between 2005 and 2009. The toe was intact in July 2005, but satellite imagery dating to 2009 shows numerous icebergs floating in the ice-marginal lake, the largest having a length of more than 500 m. The calving is thought to be due to a combination of glacier retreat and the steep topography in the zone of calving.

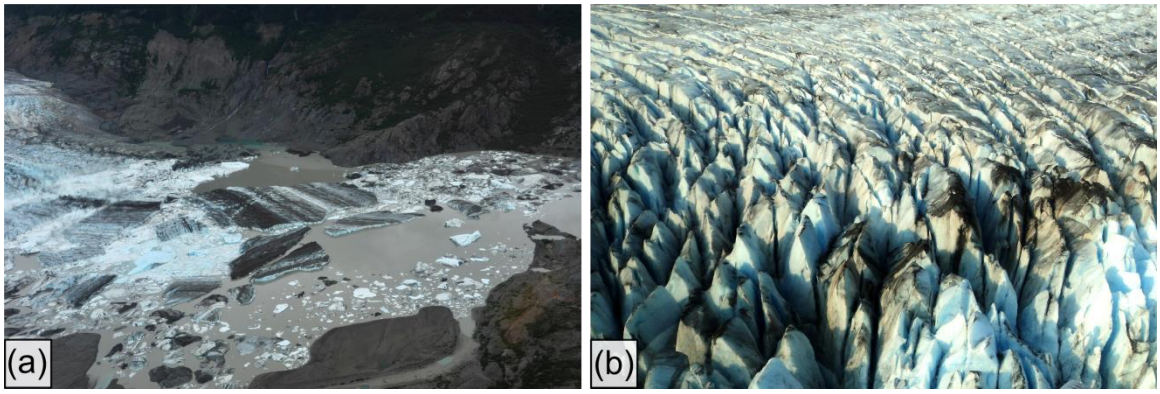

Figure 5.8: (a) Frank Mackie Glacier calving at its terminus. (b) Chevron crevasses in Frank Mackie Glacier. Photos taken July 2013.

Sample Sites

Site 1- Lower moraine: The crest of the lower south lateral moraine is at ~725 m asl (Figure 5.9). Wood was collected between 700 to 720m asl, in a large, bowl-shaped gully experiencing retrogressive mass wasting and debris flow activity (Figure 5.10a and 5.10b). Many of the largest boles collected from debris flow deposits have overgrown avalanche scars.

The lower south lateral moraine is composed of several stratigraphic units and three woody layers (WL) (Figure 5.11). At 700 m asl, below the bottom till unit, WL1 consists of a black, hummocky organic horizon. Three in-situ boles were sampled from WL1 (FM0501# 01 to 03). FM0501-03 returned a C^{14} age of 1760 ± 40 yrs BP. In addition, three in-situ boles (FM0501# 04 to 06) were found in upright growth position above WL1 at 705 m asl. FM0501-04 provided a C^{14} age of 870 ± 30 yrs BP and FM0501-06 yielded a ^{14}C age of 560 ± 30 yrs BP (Table 5.2).

A bole (FM0501-07) was recovered from a clay lens below WL2 and is considered in-situ. A detrital sample (FM0501-08) was found directly above the clay layer. Detrital wood was found in a sand lens in WL2 at 715 m asl (FM0501-09). A single in-situ sample (FM0501-10) collected from WL2 gave a ^{14}C age of 860 ± 30

yrs BP (Table 5.2). WL3 comprises logs in till at 720 m asl near the top of the moraine. Three in-situ and one detrital samples (FM0501# 11-14) were retrieved from WL3 near the top side of the bowl-shaped gully.

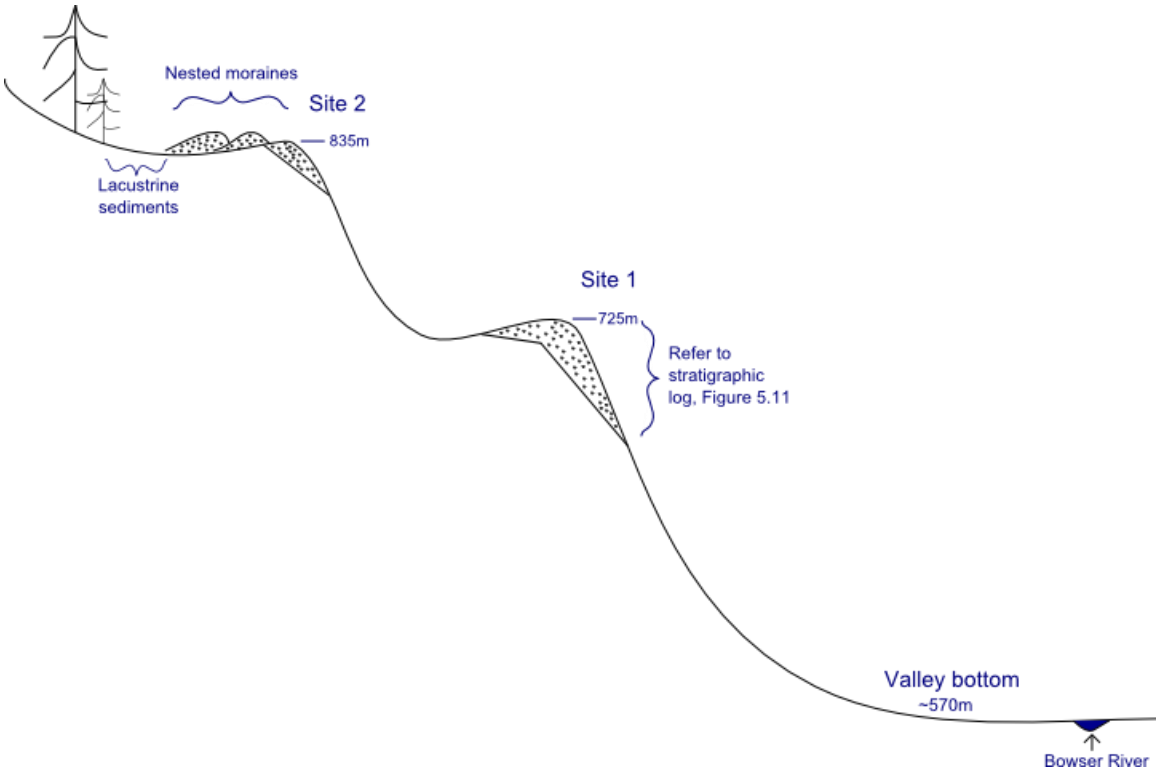

Figure 5.9: Overview of valley wall south of Frank Mackie Glacier (not to scale).

Figure 5.10: (a) The mass wasting zone of site 1 at Frank Mackie Glacier. (b) View down the gully at site 1.

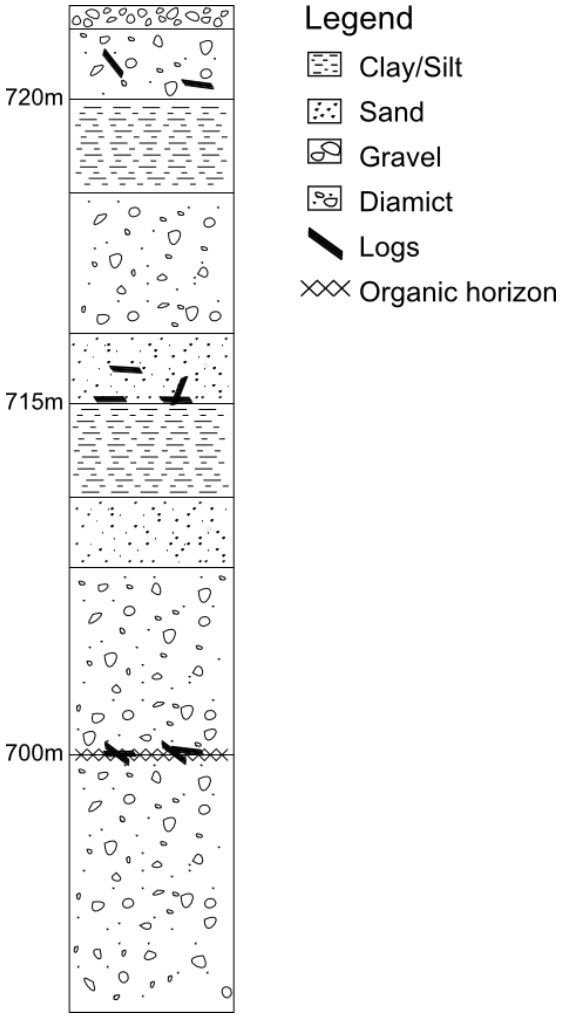

Figure 5.11: Stratigraphic section of the southern lower moraine of Frank Mackie Glacier (site 1) (Figure not to scale).

Site 2 - Upper moraine: A set of three nested moraines are found in the upper moraine site in front of the trim line (Figure 5.9). Lacustrine sediments were on the surface past the trim line. The crest of the most proximal moraine has an elevation of ~835m asl. The largely unvegetated area between the lower (site 1) and upper (site 2) moraines is gently sloping and basin-shaped (Figure 5.12b). It is likely that a confluent cirque glacier occupied the upper area, interacting with Frank Mackie Glacier during periods of advance. This ablated glacier is informally referred to as

Junior Glacier. Due to the complex interaction between Frank Mackie and Junior glaciers, stratigraphy could not be determined.

A gully intersected the nested moraines revealing a massive till unit with two woody layers in the most proximal moraine (Figure 5.12a). The upper woody layers was buried in red clay. Ten in-situ (FM0502# 01 to 06, 09 to 10, 12) and four detrital (FM0501# 07, 11, 13, 14) samples were collected between an elevation of 808 and 818 m asl. Samples site 2 were assumed to be young and therefore were not sent in for radiocarbon dating.

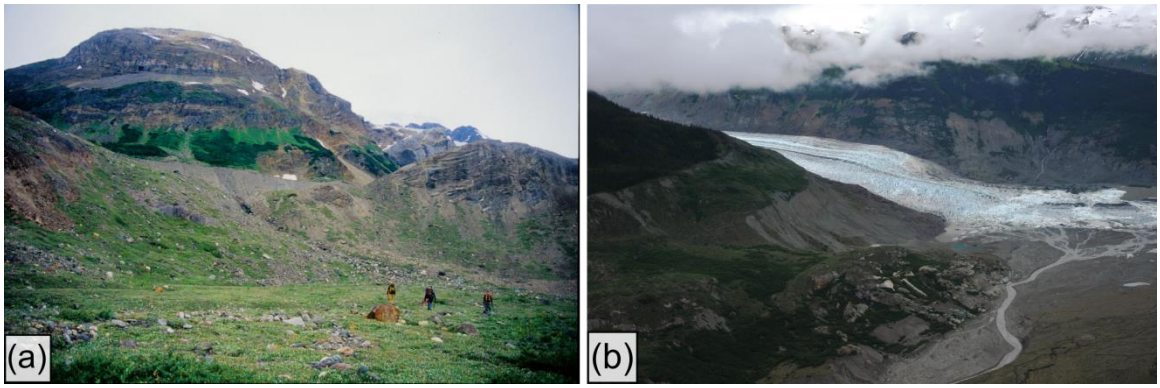

Figure 5.12: (a) Upper moraine at Frank Mackie Glacier (site 2). (b) Frank Mackie Glacier.

Site 3 - Spill area: Site 3 comprises the moraine complex below site 1. Twenty six surface samples (FM05# A-Z) were collected between 580 and 680 m asl, and ten samples were collected between 620 and 700m asl northwest of site 1 (FM05#AA-JJ).

Site 5 - North lateral moraine: Two in-situ samples at 757 and 755 m asl were found in an organic mat with visible fir needles. Sample FM05-23 returned a ^{14}C age of 2380 ±40 and sample FM05-24 gave a ^{14}C age of 2490 ±40 (Table 5.2). The logs were oriented in the direction of glacier flow. The wood mat was found in a valley-wall enclave where sediments and trees had been compacted by the glacier moving

by it (Figures 5.13a and 5.14b). Below the till is an organic mat, likely the remnants of a forest floor with a compact B horizon.

Site 6 - Spill area below north lateral moraine: Site 6 is a large gully in the north lateral moraine. Over 50 detrital samples were collected at approximately 670-685 m asl from the outwash zone of this gully.

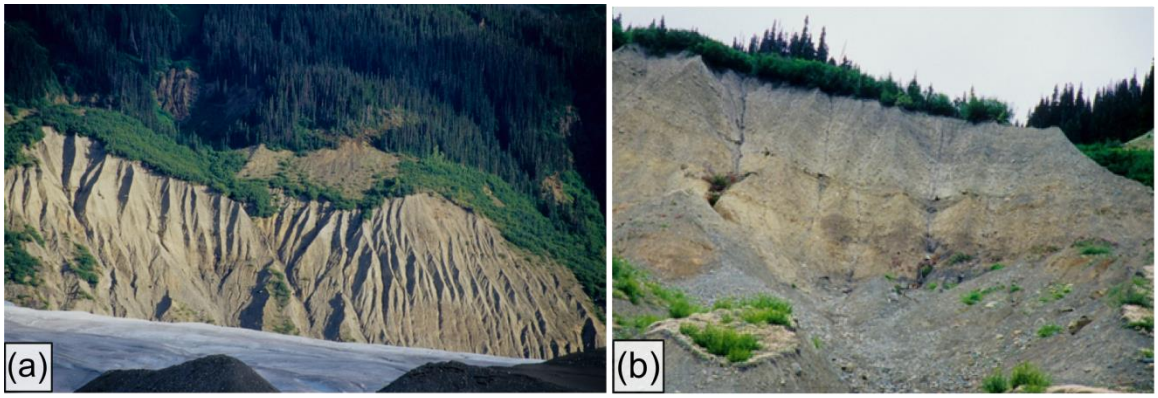

Figure 5.13: (a) North lateral moraine of Frank Mackie Glacier. (b) North lateral moraine (site 5).

5.2.4 Salmon Glacier

The area east of the northern terminus of Salmon Glacier was surveyed. The site is 100 m above the bed of Summit Lake and approximately 1 km northeast of the present northern terminus of the glacier. A single in-situ bole (SG-01), with a C^{14} age of 4950 ± 30 yrs BP, was found partially submerged in a small pond, proximal to a partially vegetated, 1.5 m high moraine (Table 5.2, Figures 5.14a and 5.14b). One end of the bole was buried beneath vegetated soil and boulders. Other nearby ponds contained fallen boles, however there were no indications that they had been placed or killed by glacier advance and thus were assumed to have died and fallen in the ponds naturally.

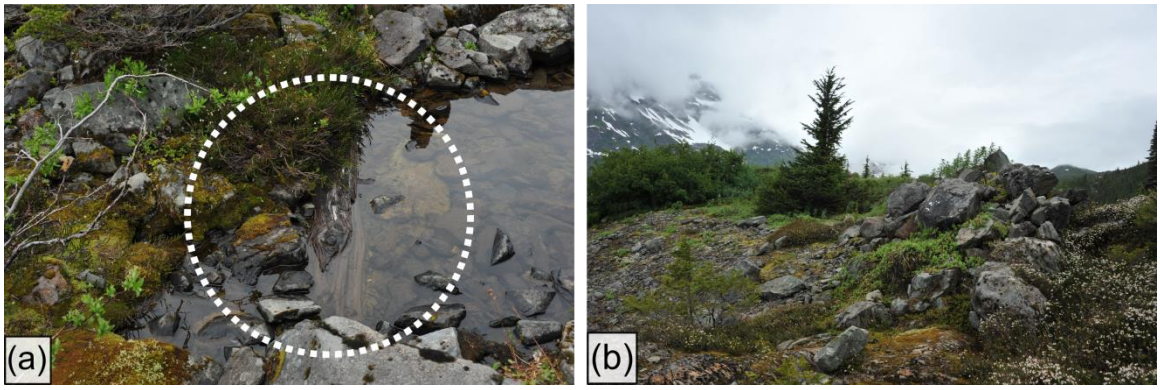

Figure 5.14: (a) Partially submerged and buried bole, SG13-01. (b) Moraine at the northern terminus of Salmon Glacier, facing north.

5.3 Dendrochronological Results

A total of 156 samples were collected from the field prepared in the lab. Approximately one third of samples could not be internally cross-dated (Appendix Table B.1). A number of these were discarded following coarse-grit sanding as they contained too few rings (<50) to enable cross-dating. The remainder of samples which could not be internally cross-dated was due to extensive reaction wood, significant rot, and/or abnormal growth throughout the samples. 84 samples achieved internal cross-dating correlations of ≥0.400 and could be used for constructing floating chronologies (Appendix Table B.1).

Eight floating chronologies (Bowser 1-8) were cross-dated to anchored radiocarbon-dated samples (Table 5.3). Interseries correlations ranged from 0.435 to 0.470, indicating they are suitable for cross-dating. Average mean sensitivity for the chronologies ranges from 0.142 to 0.237. These low to intermediate values suggest that the subalpine fir and mountain hemlock samples are fairly complacent indicating that variation in tree-ring width may be dominated by factors other than climate. Two floating chronologies (Bowser 9 and 10) were cross-dated to subalpine

fir and mountain hemlock living tree chronologies from Surprise Glacier (Jackson et al., 2008).

Floating chronologies (Bowser 1-8) were anchored to the mean of the calibrated radiocarbon age (Figure 5.15). Although calibrated ages are non-Gaussian, the mean calibrated age was selected to pin the floating chronologies. Error bars adjacent to the sample represent the range of ages the sample may fall into. The calibrated ages were used in lieu of conventional ages to allow for comparison between the anchored floating chronologies to those which cross-dated with living chronologies (Bowser 9-10).

Details of the subfossil chronologies are presented in Appendix Tables B.2 and B.3. Most of the samples collected in the field did not cross-date to existing living tree chronologies of subalpine fir and mountain hemlock from Frank Mackie Glacier site (UVTRL, *unpublished*). Many samples from Charlie Glacier could not be used for cross-dating, because they contained either too few rings or too much reaction wood.

Table 5.3: Summary of subfossil floating chronologies.

Floating chronology name	No. of subfossil samples	Interval (cal. years BP)	Total length (years)	Pearson's r value	Mean sensit-ivity	14C samples	Living tree chron. x-dated to*
Bowser 1	3	5444-5210	234	0.470	0.237	CAN06-11	
Bowser 2	5	3613-3369	244	0.450	0.227	CAN06-01	
Bowser 3	7	3549-3227	322	0.444	0.191	KG13-01	
Bowser 4	5	2938-2687	251	0.455	0.206	KG13-30	
Bowser 5	7	2633-2394	239	0.447	0.195	FM05-23, FM05-24	
Bowser 6	5	1961-1673	288	0.443	0.199	FM05-0103	
Bowser 7	11	956-612	344	0.435	0.189	FM05-0104	
Bowser 8	5	629-428	201	0.457	0.196	KG13-26	
Bowser 9	9	322-121	201	0.529	0.189	-	SuG-SAF
Bowser 10	6	416-128	288	0.508	0.219	-	SuG-MH

*Surprise Glacier living tree chronologies were built by Jackson et al. (2008). SAF=subalpine fir and MH=mountain hemlock.

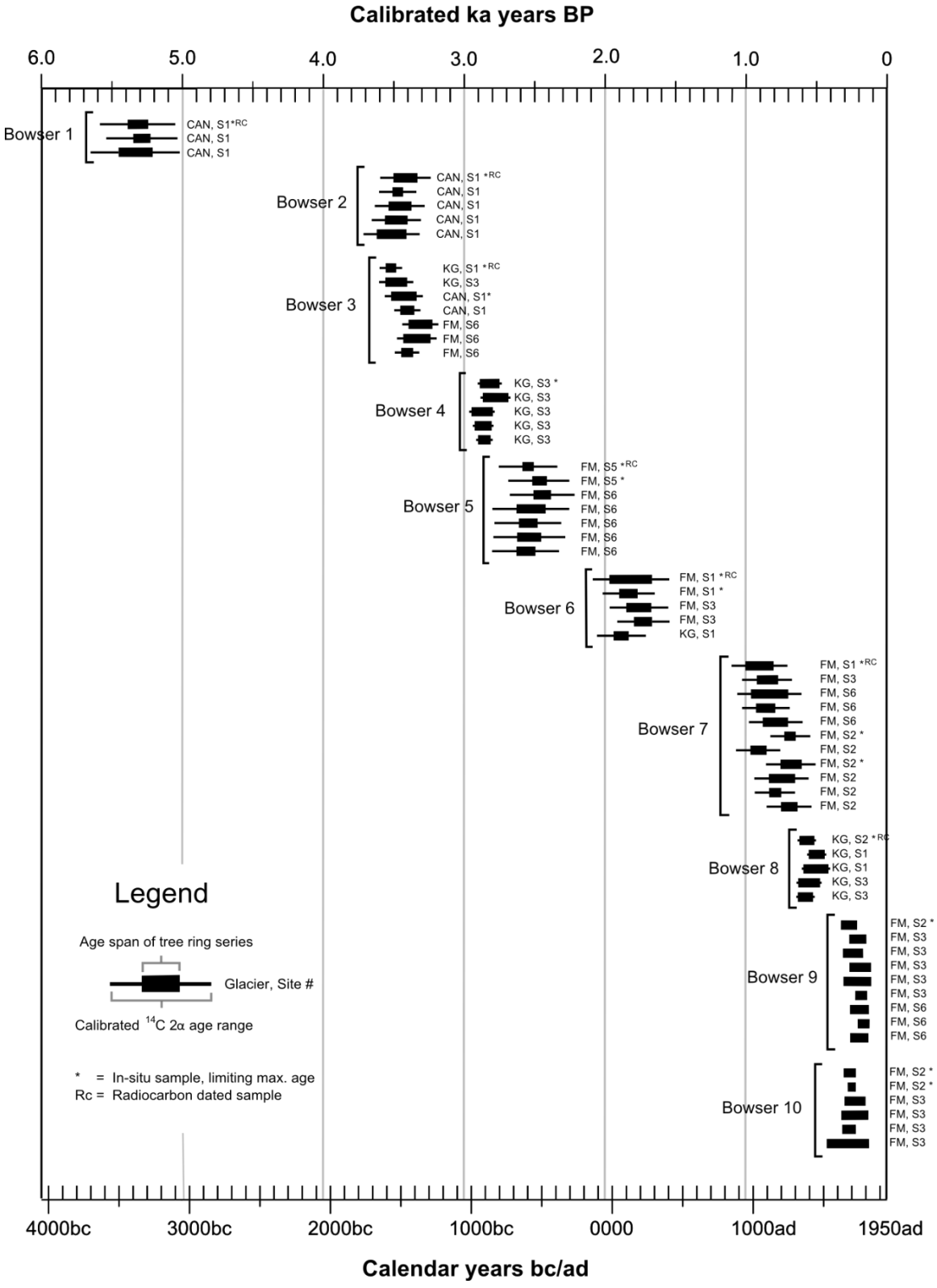
Calibrated ka years BP
6.0
5.0
4.0
3.0
2.0
1.0
0
Bowser 1
CAN, S1*RC
CAN, S1
CAN, S1
Bowser 2
CAN, S1 *RC
CAN, S1
CAN, S1
CAN, S1
CAN, S1
Bowser 3
KG, S1 *RC
KG, S3
CAN, S1*
CAN, S1
FM, S6
FM, S6
FM, S6
Bowser 4
KG, S3 *
KG, S3
KG, S3
KG, S3
KG, S3
Bowser 5
FM, S5 *RC
FM, S5 *
FM, S6
FM, S6
FM, S6
FM, S6
FM, S6
Bowser 6
FM, S1 *RC
FM, S1 *
FM, S3
FM, S3
KG, S1
Bowser 7
FM, S1 *RC
FM, S3
FM, S6
FM, S6
FM, S6
FM, S2 *
FM, S2
FM, S2 *
FM, S2
FM, S2
FM, S2
Bowser 8
KG, S2 *RC
KG, S1
KG, S1
KG, S3
KG, S3
Bowser 9
FM, S2 *
FM, S3
FM, S3
FM, S3
FM, S3
FM, S3
FM, S6
FM, S6
FM, S6
Bowser 10
FM, S2 *
FM, S2 *
FM, S3
FM, S3
FM, S3
FM, S3
Legend
Age span of tree ring series
Glacier, Site #
Calibrated 14C 2α age range
* = In-situ sample, limiting max. age
Rc = Radiocarbon dated sample
4000bc
3000bc
2000bc
1000bc
0000
1000ad
1950ad
Calendar years bc/ad

Figure 5.15: (preceding page) Subfossil tree chronologies constructed from sites in the Bowser River Watershed. Cross-dated samples are grouped with brackets. Each rectangle represents the temporal extent of a sample. Error bars for Bowser 1-8 represent the range of ages which the sample fall on, and are based on radiocarbon dated sample, denoted by * Bowser 9 and 10 are cross-dated to living tree chronologies. Refer to Appendix A in regards to methodology used for anchoring floating chronologies with radiocarbon dates.

Chapter 6: Discussion

6.1 Interpretation of the Bowser River Watershed Glacier Record

6.1.1 Charlie Glacier

Remains of forests disturbed by the early Tiedemann Advance at Charlie Glacier were found pressed against bedrock by the expanding glacier margin at several sites, and also contained in the lowest wood mat at site 3. Evidence for the late Tiedemann Advance was determined from radiocarbon-dated boles in a wood mat located at a higher elevation. These samples indicate that Charlie Glacier advanced into valley side forests at least two times during the Tiedemann interval. The samples dated to early Tiedemann were found at an elevation of 140 m above Chas Lake and approximately 350 m away from current terminus of the glacier. This evidence shows that glacier mass balance during the Tiedemann Advance was much more positive than it is today.

A single in-situ LIA stump with a date of 540-500 cal. yr BP was found on the distal side of the lateral moraine. The sample was located close to the valley wall, and separated from Charlie Glacier by a well-defined moraine with a sharp crest. This second moraine indicates that Charlie Glacier advanced multiple times during the LIA.

Several surface samples from sites 1 and 3 cross-date to the LIA (Figure 5.12). No samples from Charlie Glacier were radiocarbon dated to the FMA, although one sample cross-dated with the FMA floating chronology, consisting mainly of samples from Frank Mackie Glacier. It is likely that the lack of in-situ evidence for

LIA and FMA advances at Charlie Glacier is due to the extensive erosion and downwasting of the moraines since these advances.

The exposed slope at site 3 extends more than 700 m away from the current terminus of Charlie Glacier, likely marking the farthest extent of Charlie Glacier during the LIA. The downvalley end of the exposed slope is approximately 250 m beyond where in-situ late and early Tiedemann samples were found, indicating that the most recent advance of Charlie Glacier has been the largest.

6.1.2 Canoe Glacier

Radiocarbon and dendrochronological dating of Canoe Glacier samples taken from two wood mats provides evidence for advances at 5444-5210 and 3613-3369 cal. yr BP (Harvey et al. 2012). The lack of later Holocene advances may be due to the extensive ablation of the glacier, leading to destabilization of the lateral moraines built by more recent glaciers. The inaccessible higher wood mat at the site signifies activity of a larger glacier, which probably advanced during either the LIA or FMA.

6.1.3 Frank Mackie Glacier

The two southern moraines of Frank Mackie Glacier provide ages for the LIA and FMA. Radiocarbon ages from the lower moraine indicate that it was built by an early LIA advance at 700-900 cal. yr BP. The lower moraine also contains evidence suggesting that it was constructed during by the First Millennium AD advance at 1810-1560 cal yr BP.

The history of moraine construction by Frank Mackie Glacier is complicated by its interaction with Junior Glacier. Cross-dating of surficial samples provides support for the existence of Junior Glacier during the LIA. Kill dates for the surficial samples from the lower moraine complex (site 3) were 80 years younger than kill dates for in-situ samples at a higher elevation near the trim line (site 2). The two sets of ages record the same period of glacier advance, although Junior Glacier advanced into standing forests earlier than Frank Mackie Glacier due to its proximity to the site.

No Frank Mackie samples cross-dated with Charlie Glacier LIA samples (470 yr BP), despite the similarity in the radiocarbon ages from the two localities (Charlie Glacier, ca. 470 yr BP; Frank Mackie Glacier, ca. 560 yr BP). The different species that were sampled at the two sites may have prevented successful cross-dating. Subfossil wood samples at Frank Mackie Glacier sites 1 and 2 were mainly mountain hemlock, whereas Charlie Glacier samples were exclusively subalpine fir.

Evidence for the late Tiedemann advance at Frank Mackie Glacier was found in the north lateral moraine, close to present-day ice levels, suggesting that the late Tiedemann advance may have been smaller than the LIA and FMA advances. These findings differ from those of Clague et al. (1992) who stated that Frank Mackie Glacier was smaller during the FMA than it was during the LIA and Tiedemann Advances. Their conclusion was based on the lack of lacustrine sediments throughout the Tide Lake basin during the FMA (Clague and Mathews, 1992). Other surficial samples at the site cross-dated with samples from Canoe and Charlie glaciers to support an Early Tiedemann glacier advance.

6.1.4 Salmon Glacier

The single sample collected at Salmon Glacier (SG13-01) dated to 5750-5600 cal yr BP. Had the tree died in place, it would have most likely decayed. In this case the sample was relatively well preserved and was most likely buried in a moraine by an advancing glacier before being remobilized by subsequent advance(s). The advance that first buried the tree may be associated with a late Garibaldi Phase or younger advance.

6.1.5 Synthesis of Bowser River Watershed Glacier History

Dendroglaciological and radiocarbon results from this study, Clague and Mathews (1992), Clague et al. (2004), Harvey et al. (2012) and Jackson et al. (2008) provide evidence for five periods of Holocene glacier advance in the BRW (Figure 6.1): A late Garibaldi event (5.7-5.1 ka cal. yr BP), early and late Tiedemann Advances (3.8-3.4 and 2.8-2.2 ka cal. yr BP), First Millennium Advance (1.8-1.3 ka cal. yr BP) and LIA advances (0.9-0.1 ka cal. yr BP). Synchronicity in the timing of glacial events for the Bowser River Watershed glaciers will be discussed in Chapter 7: Regional Synthesis.

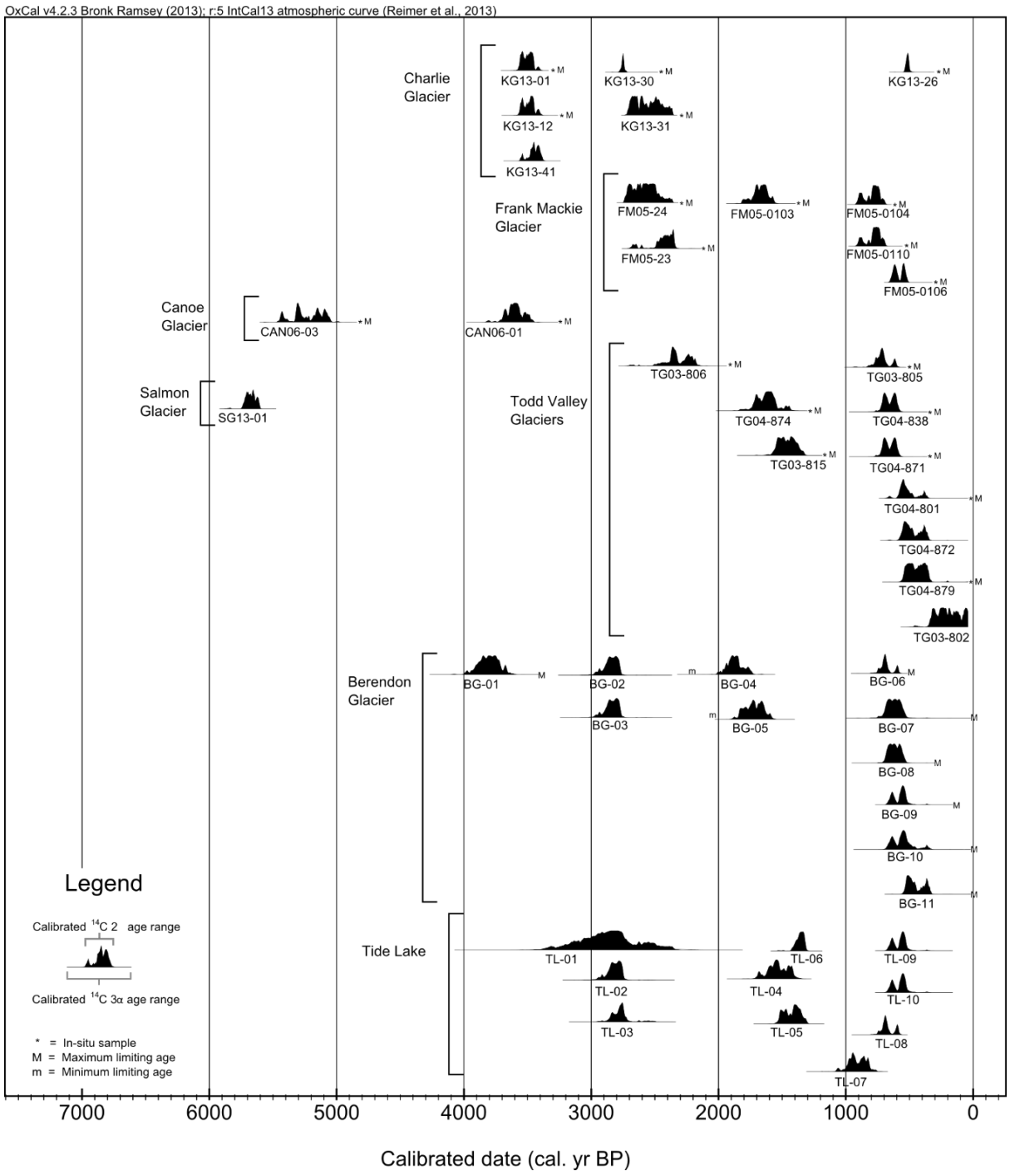

Figure 6.1: Synthesis of Bowser River Watershed radiocarbon ages. Plot outputs and radiocarbon calibration were done using OxCal v4.2.3 (Ramsey, 2013); r:5 IntCal13 atmospheric curve (Reimer et al., 2013). Sources for glaciers are listed in Appendix Table B.4.

6.1.6 Post-LIA Glacier Mass Balance in the Bowser River Watershed

No detailed mass balance studies have been undertaken in northern BC. Nonetheless, comparison of aerial photographs, maps and other data depicting glaciers in the BRW demonstrate that these glaciers are currently retreating (Tables 6.1 and 6.2). A summary of the annual retreat rates for select glaciers demonstrates the acceleration of retreat over the past century (Table 6.1 and 6.2).

Table 6.1: Imagery used for calculating average retreat rates for select glaciers in the Bowser River Watershed.

Glaciers	Year of image/map	Image/map type	Source
Knipple &	1961	Oblique air photo	Post (1961), F3-61-120. 8-9-61
Charlie	1990	Magnetometer map	Murton (1990)
	2013	Satellite image	Google Earth, Spot
Salmon	1956	Air photo mosaic	Haumann (1960)
	1982	Landsat imagery	Beedle (2012)
	2005	Landsat imagery	Beedle (2012)
	2010	Landsat imagery	Beedle (2012)
Berendon	1905	Photograph	Clague and Mathewes (1996)
	1956	Air photo mosaic	Haumann (1960)
	1977	Report	Eyles and Rogerson (1977)
	2009	Satellite image	Google Earth, Spot
Frank	1930	Photograph	Clague and Mathewes (1996)
Mackie	1997	Air photo	30BCC97145 No. 37
	2009	Satellite image	Google Earth, Spot
	2013	Satellite image	Flash Earth (2014)
Todd, Sage,	1974	Air photo	Jackson et al. (2008), BC5604 075
Bug & Two	1997	Air photo	Jackson et al. (2008), 30BCC97143 No. 36

Table 6.2: Retreat rates for select glaciers in the Bowser River Watershed.

Glacier	Period	Total retreat per period (m)	Average rate of retreat (m/yr)
Knipple	1961-1990	122	4.2
	1990-2013	1188	52
Charlie	1961-1990	0	0
	1990-2013	710-1100	31-48
Salmon	1956-1982	1430	55
(South terminus)	1982-2005	2752	120
	2005-2010	951	190
(North terminus)	1982-2005	450	19.6
	2005-2010	100	20
Berendon	1905-1956	249	4.9
	1956-1977	330	15.7
	1977-2009	800	25
Frank	1930-1997	200	3.0
Mackie	1997-2009	342-700	29-58
	2009-2013	500-888	125-222
Todd Glacier	1974-1997	1748	76
Sage Glacier	1974-1997	1104	48
Bug Glacier	1974-1997	207	9
Two Glaciers	1974-1997	805	35

Chapter 7: Regional Synthesis

7.1 Introduction

Investigations in the BRW and at other sites in the region enable a reconstruction of mid- to late Holocene glacier activity in the northern Coast Mountains. The periodicity of glacier advances in the northern BC Coast Mountains is cyclical throughout the Neoglacial period, with on average one advance per millennium, although the advances are not uniformly spaced (Figure 7.1). Millennial-scale cycling is apparent in cores from the North Atlantic Ocean, where multi-proxy data including oxygen isotopes and marine sediments, provide evidence for a cyclicity of approximately 1470 ± 500 yr (Bond et al., 1997). No single climate forcing mechanism has been found to correlate to millennial scale cycling taking place during the Holocene (Bond et al., 2007; Mayewski et al., 2005). Century-scale oscillations in climate are likely connected to variations in solar irradiance (Blaauw et al., 2004; Steinhilber et al., 2009), which affect the position and intensity of the Aleutian low pressure system (Heusser et al., 1985). Along the north Pacific Coast, the Aleutian low shifted east and further intensified at the commencement of the late Holocene, leading to increased winter precipitation (Barron and Anderson, 2011). The increase in precipitation as snowfall from the mid-to late Holocene may be responsible for the observed trend of each glacier advance being progressively larger than its immediate predecessor (Figure 7.1).

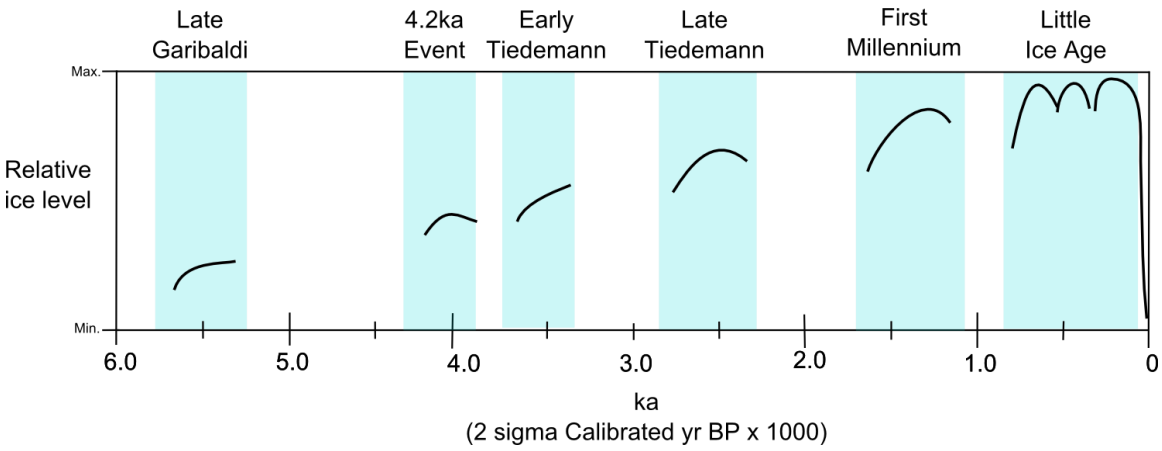

Figure 7.1: Glacier advances and relative ice levels in northern BC based on Figure 7.2.

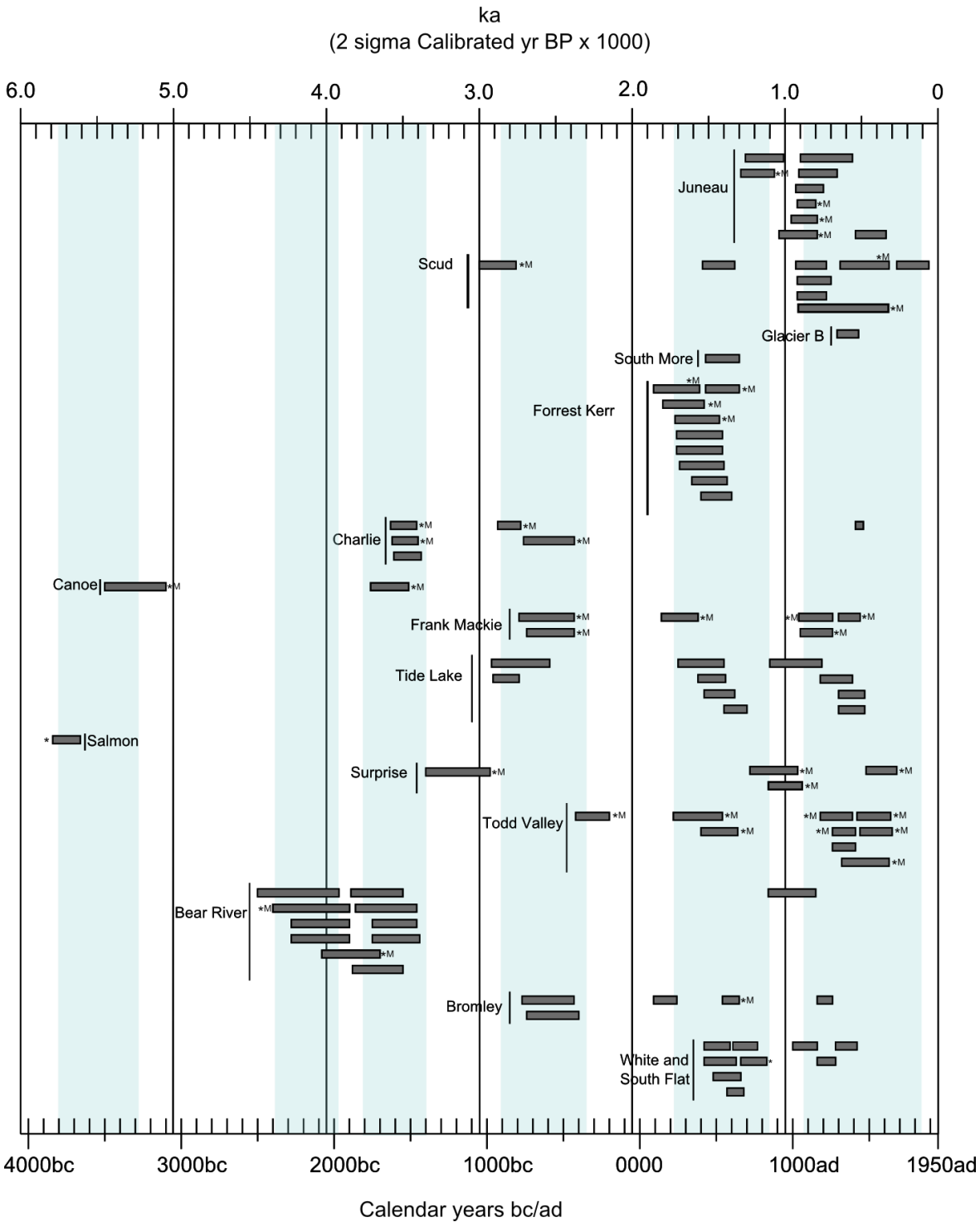

Figure 7.2: Radiocarbon-dated periods of glacier advance in northern British Columbia. Glacier sites arranged from north to south. Asterisks denote in-situ sample. Maximum limiting ages are indicated with an 'M'. Sources for glacier are listed in Appendix Table B.4.

7.2 Early Holocene

No evidence of early Holocene glacial advances has been found in the northern Coast Mountains. Evidence for the 8200-year event has been found in southern BC (Menounos et al., 2004), Alaska (Lawson et al., 2007), and the north Cascade Range, Washington (Beget, 1981), thus it seems likely that glaciers in the northern Coast Mountains also advanced at this time. The 8200-year event either did not produce significant evidence in this region or, more likely, the larger, subsequent advances destroyed the evidence for most early Holocene advances.

7.3 Mid-Holocene

Garibaldi Advance

The radiocarbon-dated log from Salmon Glacier (5740-5600 cal. yr BP) provides evidence for a mid-Holocene glacier advance in northern BC. Although the sample has uncertain provenance, a slightly younger date (5450-5050 cal. yr BP) from an organic wood mat at nearby Canoe Glacier (Harvey et al., 2012) supports evidence for glacier expansion during the mid-Holocene. Pollen analysis and lacustrine sediments records from northern BC demonstrate that the climate was cooler and wetter at this time than in the early Holocene, although warmer than in the late Holocene (Spooner et al., 2002).

The radiocarbon ages from Salmon and Canoe glaciers coincide with the end of Garibaldi Phase of glacier expansion between 6000 and 5000 ^{14}C yr BP (6.95-5.62 ka cal. yr BP) (Ryder and Thomson, 1986). The date from Canoe Glacier extends beyond the age range for the Garibaldi Phase as defined by Ryder and Thomson,

although the event did not necessarily end at 5.62 ka BP. This point is discussed by Menounos et al. (2009), who extended the period of the Garibaldi Phase by several hundred years based on evidence from the southern Coast Mountains. Yet there are few other sites that provide evidence for an advance this late during the Garibaldi Phase in the literature.

4.2 ka Advance

Evidence for glacier expansion at 4.2 ka in northern BC is limited to Bear River Glacier. A log from the lowest wood mat at 435 m asl in the moraine was radiocarbon dated at 4160-3850 cal. yr BP (Jackson et al., 2008). Additional detrital wood from higher wood mats at approximately 450 m asl provided radiocarbon ages of 4380-3820, 3980-3670, 3780-3730, 4250-3860 and 4160-3850 cal. yr BP (Osborn et al., 2013). Till beneath these wood mats may date to the Garibaldi Phase (Osborn et al., 2013). Osborn et al. (2013) also linked a third wood mat, found farther from the glacier terminus at a higher elevation, to a larger glacier expansion during early Tiedemann period.

7.4 Late Holocene

Tiedemann Advances

A glacier advance during the early Tiedemann period, at 3.7 ka cal. yr BP, is strongly supported by evidence from the BRW (Harvey et al., 2012) and Bear River Glacier (Jackson et al., 2008; Osborn et al., 2013). During the late Tiedemann period, between 2.9 and 2.25 ka, glaciers readvanced past their early Tiedemann extents. Evidence for late Tiedemann glacier activity is extensive and has been reported at

Tide Lake (Clague and Mathews, 1992) and Scud (Pietrusiak, 2012), Bromley (Hoffman and Smith, 2013) Todd (Jackson et al., 2008), Frank Mackie and Charlie glaciers.

The length of time between the two Tiedemann events suggests they are distinct and should be treated as separate advances. Following the early Tiedemann advance, temperatures were favourable for establishing valley-side forests with trees of at least 200 years in age and the rudimentary development of soil at Charlie Glacier.

First Millennium AD Advance

Evidence for the FMA advance in this region spans close to 700 years (Figure 7.1b). On average, glaciers closer to the coast (Berendon, Forrest Kerr, Frank Mackie and Salmon) appear to have advanced earlier in the FMA than glaciers farther east (White, South Flat and Surprise glaciers, and Juneau Icefield). The temporal variation in coastal vs. more continental FMA dates is approximately 200 years. However, the number of glaciers providing support for this lag is limited. There were no visible north-to-south trends in the timing of glacier episodes.

It is uncertain if the FMA was a single event or, like the LIA, comprised numerous, closely spaced advances. Tide Lake and Forrest Kerr, White and South Flat glaciers demonstrate that there may have been at least two separate glacier advances during the FMA. Jackson et al. (2008) suggested that Surprise Glacier may record two separate events, however their calibrated ages on the two advances overlap.

Little Ice Age Advances

The LIA history of North America is complex, with numerous phases of glacier expansion. In the BRW, the oldest LIA advance appears to have occurred earlier at Frank Mackie Glacier than Charlie or Todd Valley glaciers (Figure 7.1b). It may be that Frank Mackie Glacier's gently sloping topography aided in retaining detrital wood in its stratigraphy of the lower southern moraine. The growth of Junior Glacier likely affected the construction of the Frank Mackie moraine. Scud Glacier (Petrusiak, 2012) and glaciers emanating from the Juneau Icefield (Clague et al., 2010) also record an early LIA advance beginning ~900 cal. yr BP (1050 AD).

Todd Valley glaciers, including Todd, Sage and Two glaciers, coalesced to occupy the valley at 700-600 cal. yr BP (1250-1350 AD) (Jackson et al., 2008). Frank Mackie, Glacier B (UVTRL, unpublished), Bromley (Hoffman and Smith, 2013), White and South Flat (Johnson and Smith, 2012) glaciers and Tide Lake (Clague and Mathews, 1992) also record an advance during this period. Another period of glacier expansion soon followed at around 500 cal. yr BP (1450 AD) at Charlie, Scud and Todd Valley and at glaciers flowing from the Juneau Icefield.

In southern and central BC the LIA maximum occurred between 150 and 50 cal. yr BP (1800-1900 AD) (Desloges and Ryder, 1990; Smith and Laroque, 1996). Similar evidence is found in the northern Coast Mountains. The outer, sharp-crested lateral moraine at Charlie Glacier was built following deposition and burial of the 560 cal. yr BP (1390 AD) log of the innermost moraine. At Surprise Glaciers, logs buried beneath the moraine crest yielded ages of 204-107 cal. yr BP (1746-1843 AD) (Jackson et al., 2008). Similarly at Todd Glacier, several logs which had been

mobilized by the glacier and pushed into a detrital pile were cross-dated to a living tree chronology to 1898 A.D. (Jackson et al., 2008). The late date for a LIA advance of Todd Glacier agrees with findings of Haumann (1960) who stated that Salmon Glacier sat at its LIA maximum until approximately AD 1920.

Both Scud and Todd Valley glaciers record three moraine-building events during the LIA, although Todd Valley does not record the earliest LIA event. In northern BC there may have been a total of four, regionally synchronous periods of glacier expansion during the LIA. An alternative interpretation is that there were three events, with different timing among the sites.

7.5 Summary of Northern Coast Mountain Glacier Advances

Northern Coast Mountain glaciers provide evidence for six periods of glacier advance in the mid- to late Holocene: late Garibaldi, 4.2 ka, early and late Tiedemann, First Millennium AD and the Little Ice Age. The timing of these advances is similar to that in the southern and central Coast Mountains (Menounos et al., 2009) and Cariboo Mountains (Maurer et al., 2012). These findings improve our knowledge of the timing and complexity of glacier activity in northwest North America by confirming that the advances were regional, and the climatic regimes influencing growth and decay affected the entire length of the Coast Mountains. A shift in the Aleutian Low may explain the increased frequency of glacier advances during the Late Holocene; however improved resolution of mid-Holocene glacier history is needed to support this theory.

The precision of the radiocarbon ages is low for many of my samples due to limitations in the accuracy of radiometric dating, as well as fluctuations in atmospheric carbon levels during certain periods. Radiometric dating has become significantly more precise over the past few decades, however previously dated material cannot be redated due to issues of contamination and/or sample destruction during the dating process. While revisiting glacier field sites is possible, not all wood mats and in-situ boles may be intact as many of the sites for dendroglaciological investigations are typically found on steep sided moraines, which are susceptible to erosion and mass wasting events. Further, the costs associated with radiometric dating and returning to field sites may be prohibitive in some cases. Although a radiocarbon age provides an approximate date for an event, it has inherent instrumental uncertainty and calibration that may increase uncertainty by up to several hundred years, making it much more challenging to pinpoint the exact time of a single advance. A minimum age of an advance can be found by dating living trees that recolonize moraines following retreat. Limitations for this type of dating are that it requires the oldest tree on the moraine to be samples and requires factoring in the ecesis interval (Coulthard and Smith, 2013b).

Dendrochronological cross-dating of samples to living tree chronologies provides a precise calendar date for tree death. Unfortunately most living chronologies in northern BC extend back to only 400 years, limiting the use of this technique. The anchoring of floating chronologies through radiocarbon dating of in-situ samples is useful because it provides support for the inference that cross-dated

surficial samples were also killed by the glacier, rather than by mass movement events.

Chapter 8: Conclusions

8.1 Summary

Five periods of glacier advance are recognized in the BRW: (1) a late Garibaldi Advance at 5.7-5.2 ka cal. yr BP; (2) an early Tiedemann Advance at 3.8-3.4 ka cal. yr BP; (3) a late Tiedemann Advance at 2.8-2.2ka cal. yr BP; (4) a First Millennium AD Advance with two phases at 1.8-1.3 ka cal. yr BP; and (5) three or four LIA events at 0.9-0.1 ka cal. yr BP. The timing and extents of Holocene glacier advances in the BRW are comparable with those reported by others in the BC Coast Mountains. Glacier advances in the BRW were episodic, with each subsequent advance progressively larger than the preceding advance. Cross-dating and radiocarbon dating of samples from many glacier sites enabled a more detailed chronology to be constructed than would have been possible at a single site.

8.2 Limitations and Recommendations for Future Research

Limitations of this research included working with different tree species, resulting in some cases in an inability to cross-date samples from different sites. Many of the samples proved challenging to cross-date because they contained reaction wood. The condition of the samples reflects the steep slopes and harsh environment in which the trees live.

The cyclical retreat and advance of glaciers enabled the preservation of multiple wood mats and construction of several floating chronologies. As the living chronologies for subalpine fir and mountain hemlock in this region only extend to

300-400 cal. yrs BP, the majority of the floating chronologies cannot be cross-dated into a master chronology. Cross-dating floating chronologies to a master chronology allows for far greater accuracy than radiocarbon dating in determining the timing of glacier advances. The living chronology record in the region could be extended by collecting coarse woody debris submerged in lakes, as these remains can be preserved for several thousand years (Eronen et al., 2002; Pitman and Smith, 2012).

Cores from lakes might provide further insights into Holocene glacier activity and long-term climatic trends for the region. Both small proglacial lakes, such as Chas Lake and larger lakes, such as the Bowser Lake, might provide insights into past glacier and climate dynamics (Gilbert et al., 1997; Vasskog et al., 2012).

Current nomenclature used for glacier advances remains problematic. Further studies on comparing maritime and continental glacier histories are necessary to demonstrate if there are differences in the timing of glacier advances that might reflect differences in climate forcing mechanisms.

References

Adams J, Maslin M and Thomas E (1999) Sudden climate transitions during the Quaternary. *Progress in Physical Geography* 23: 1–36.

Aldrick DJ (1988) Volcanic centres in the Stewart Complex (103P AND 104A,B). *British Columbia Energy, Mines and Petroleum Resources Geologic Fieldwork, Paper* 1989-1, 233-240.

Allen SM and Smith DJ (2007) Late Holocene glacial activity of Bridge Glacier, British Columbia Coast Mountains. *Canadian Journal of Earth Sciences* 44: 1753–1773.

Alley RB and Agustsdottir A (2005) The 8k event: cause and consequences of a major Holocene abrupt climate change. *Quaternary Science Reviews* 24: 1123–1149.

Alley RB, Mayewski PA, Sowers T, Stuiver M, Taylor KC and Clark PU (1997) Holocene climatic instability: A prominent, widespread event 8200 yr ago. *Geology* 25: 483-486.

Barclay DJ, Wiles GC, and Calkin PE (2009) Holocene glacier fluctuations in Alaska. *Quaternary Science Reviews* 28: 2034-2048.

Barron JA and Anderson L (2011) Enhanced Late Holocene ENSO/PDO expression along the margins of the eastern North Pacific. *Quaternary International* 235: 3–12.

Barry RG (2006) The status of research on glaciers and global glacier recession: a review. *Progress in Physical Geography* 30: 285–306.

Beedle MJ (2012) Salmon Glacier extents: 1982-2010. In: *Glacier Change*. Available at: www.glacierchange.org (accessed 02 February 2014).

Beget JE (1981) Early Holocene glacier advance in North Cascade Range, Washington. *Geology* 9: 409-413.

Blaauw M, van Geel V, van der Plitch J (2004) Solar forcing of climactic change during the mid-Holocene: Indications from raised bogs in the Netherlands. *The Holocene* 14: 35-44.

Bond G, Showers, W, Chesby M, Lotti R, Almasi P, deMenocal P, Priore P, Cullen H, Hajdas I and Bonani G (1997) A pervasive millennial-scale cycle in North Atlantic Holocene and glacial climates. *Science* 278: 1257-1266.

British Columbia Ministry of Environment (2013) Ecoregion unit descriptions. Province of British Columbia. Available at: www.env.gov.bc.ca/ecology/ecoregions/humidtemp.html (accessed 30 March 2013).

Broeker WS, Bond G, Klas M, Bonani G, Wolfli W (1990) A salt oscillator in the Atlantic? 1. The concept. *Paleoceanography* 5: 469-477.

Bunbury J and Gajewski K (2009) Postglacial climates inferred from a lake at treeline, southwest Yukon Territory, Canada. *Quaternary Science Reviews* 28: 354-369.

Clague JJ (1989) Quaternary geology of the Canadian Cordillera. In: Fulton, R.J. (Ed.), Quaternary Geology of Canada and Greenland. Geology of Canada, 1. Geological Survey of Canada, pp. 15–96.

Clague JJ (2000) Recognizing order in chaotic sequences of Quaternary sediments in the Canadian Cordillera. *Quaternary International* 68-71: 29–38.

Clague JJ and Mathewes RW (1996) Neoglaciation, glacier-dammed lakes and vegetation change in northwestern British Columbia, Canada. *Arctic and Alpine Research* 28: 10–24.

Clague JJ and Mathews WH (1992) The sedimentary record and Neoglacial history of Tide Lake, northwestern British Columbia. *Canadian Journal of Earth Sciences* 29: 2383–2396.

Clague JJ, Koch J and Geertsema M (2010) Expansion of outlet glaciers of the Juneau Icefield in northwest British Columbia during the past two millennia. *The Holocene* 20: 447–461.

Clague JJ, Menounos B, Osborn G, Luckman BH and Koch J (2009) Nomenclature and resolution in Holocene glacial chronologies. *Quaternary Science Reviews* 28: 2231–2238.

Clague JJ, Wohlfarth B, Ayotte J, Eriksson M, Hutchinson I, Mathewes RW, Walker IR and Walker L (2004) Late Holocene environmental change at treeline in the northern Coast Mountains, British Columbia, Canada. *Quaternary Science Reviews* 23: 2413–2431.

Clark GKC and Holdsworth G (2002) Glaciers in the Coast Mountains. In: *Glaciers of North America.* U.S. Geological Survey Professional Paper 1386–J–1, pp. 290-300.

Coulthard BL and Smith DJ (2013b) Dendroglaciology. In: Elias S.A. (eds) *The Encyclopedia of Quaternary Science.* Amsterdam: Elsevier, vol. 2, pp. 104-111.

Cremonese D (1986) *Assessment Report on the Geological and Geochemical Work on the Following Claim: Treaty 2006 (1)*. Tueton Resources Corp., Vancouver BC. Geological Branch Assessment Report 14, pp. 1-21.

Cronin TM, Vogt PR, Willard DA, Thunnell R, Halka J, and Berke M (2007) Rapid sea level rise and ice sheet response to 8,200-year climate event. *Geophysical Research Letters* 34: 1-6.

Crutzen PJ (2006) 1.2: The "Anthropocene". In: Elhers E and Krafft T(eds) *Earth System Science in the Anthropocene*. Berlin Heidelberg: Springer, pp 13-18.

Debret M, Sebag D, Crosta X, Massei N, Petit J-R, Capron E and Bout-Roumazeilles V (2009) Evidence from wavelet analysis for a mid-Holocene transition in global climate forcing. *Quaternary Science Reviews* 28: 3675-2688.

Denton GH and Karlén W (1973) Holocene climatic variations- Their pattern and possible cause. *Quaternary Research* 3: 155-205.

Desloges JR annd June JM (1990) Neoglacial history of the Coast Mountains near Bella Coola, British Columbia. *Canadian Journal of Earth Science*s 27: 281-290.

Dyurgerov MB and McCabe GJ(2006) Associations between accelerated glacier mass and wastage increased summer in coastal temperature regions. *Arctic, Antarctic, and Alpine Research* 38: 190–197.

Dyurgerov MB and Meier MF (2000) Twentieth century climate change: evidence from small glaciers. *Proceedings of the National Academy of Sciences of the United States of America* 97: 1406–1411.

Eckstein D and Pilcher JR (1990) Dendrochronology in western Europe. In: Cook ER and Kairiukstis LA (eds) *Methods of Dendrochronology:Applications in the Environmental Sciences.* Boston, MA: Kluwer Academic Publishers, pp 11–13.

Environment Canada (2014) Climate normals. National Climate Data and Information Archive. Available at: http://climate.weatheroffice.gc.ca/climate_normals/index_e.html (accessed 20 June 2014).

Eronen M, Zetterberg P, Briffa KR, Lindholm M, Meriläinen J and Timonen M (2002) The supra-long Scots pine tree-ring record for Finish Lapland: Part 1, chronology construction and initial inferences. *The Holocene* 12: 673-680.

Eyles N and Rogerson RG (1977) Artificially induced thermokarst in active glacier ice: An example from north-west British Columbia, Canada. *Journal of Glaciology* 18: 437-444.

Fisher DA and Jones SJ (1971) The possible future behaviour of Berendon Glacier, Canada- A further study. *Journal of Glaciology* 10: 85-93.

Flash Earth (2014) Bowser River Watershed, Canada. Digitial Globe, 2014. http://www.flashearth.com (Acquired 01 June 2014)

Fritz M, Kerzschuh U, Wetterich S, Lantuit H, De Pascale GP, Pollard WH and Schirrmeister L (2012) Late glacial and Holocene sedimentation, vegetation, and climate history from easternmost Beringia (northern Yukon Territory, Canada). *Quaternary Research* 78: 549-560.

Fulton RJ (1991) A conceptual model for growth and decay of the Cordilleran Ice Sheet. *Géographie physique et Quaternaire* 45: 281-286.

Galimberti M, Ramsey CB and Manning SW (2004) Wiggle-match dating of tree-ring sequences. *Radiocarbon* 46: 917-924.

Gavin DG, Henderson ACG, Westover KS, Fritz SC, Walker IR, Leng MJ and Hu FS (2011) Abrupt Holocene climate change and potential response to solar forcing in western Canada. *Quaternary Science Reviews* 30: 1243–1255.

Gilbert R, Desloges JR and Clague JJ (1997) The glacilacustrine sedimentary environment of Bowser Lake in the northern Coast Mountains of British Columbia Canada. *Journal of Paleolimnology* 17: 331–346.

Google Earth V 7.1.2.2041 (2014) Bowser River Watershed, Canada, 56°26'35.73"N, 129°58'21.45"W, eye alt 13.39km. Digital Globe 2014, http://www.earth.google.com, (accessed 21 Dec 2014).

Grissino-Mayer, HD (2001) Evaluating tree-ring accuracy: A manual and tutorial for the computer program COFECHA. *Tree-Ring Research* 57: 205-221

Grove EW (1986) Geology and Mineral Deposits of the Unik River-Salmon River-Anyox Area. *British Columbia Ministry of Energy, Mines and Petroleum Resources. Bulletin* 63:(Dec) pp 1-23.

Hanson G (1932) Varved clays of Tide Lake, British Columbia*. Transactions of the Royal Society of Canada* 26: 35-34.

Hart S, Clague, J and Smith D (2010) Dendrogeomorphic reconstruction of Little Ice Age paraglacial activity in the vicinity of the Homathko Icefield, British Columbia Coast Mountains, Canada. *Geomorphology* 121: 197-205.

Harvey JE, Smith DJ, Laxton S, Desloges J and Allen S (2012) Mid-Holocene glacier expansion between 7500 and 4000 cal. yr BP in the British Columbia Coast Mountains, Canada. *The Holocene* 22: 975–985.

Hassan G, Huang JJ, Hafez SA, Pelletier P, Armstrong T, Bown FH, Vallat CJ, Newcomen HW, Weatherly L-A and Mokos P (2012) *Technical Report and Updated Preliminary Economic Assessment of the Brucejack Project*. Report for Pretium Resources Inc. 20 February.

Haumann D (1960) Photogrammetric and glaciological studies of Salmon Glacier. *Arctic* 13: 75-110.

Hegerl GC, Zwiers FW, Braconnot P, Gillett NP, Luo Y, Marengo Orsini J-A, Nicholls N, Penner JE and Stott PA (2007) Understanding and attributing climate change. In: Climate Change 2007: The Physical Science Basis. Contribution of Working Group I to the Fourth Assessment Report of the Intergovernmental Panel on Climate Change [Solomon S, Qin D, Manning M, Chen Z, Marquis M, Averyt KB, Tignor M and. Miller HL (eds.)]. Cambridge University Press, Cambridge, United Kingdom and New York, NY, USA.

Heusser CJ, Heusser LE and Peteet DM (1985) Late-Quaternary climatic change on the North American Pacific Coast. *Nature* 315: 484-487.

Hoffman KM and Smith DJ (2013) Late Holocene glacial activity at Bromley Glacier, Cambria Icefield, northern British Columbia Coast Mountains, Canada. *Canadian Journal of Earth Sciences* 50: 599-606.

Holm K, Bovis M, and Jakob M (2004) The landslide response of alpine basins to post-Little Ice Age glacial thinning and retreat in southwestern British Columbia. *Geomorphology* 57: 201-216.

Jackson SI, Laxton SC and Smith DJ (2008) Dendroglaciological evidence for Holocene glacial advances in the Todd Icefield area, northern British Columbia Coast Mountains. *Canadian Journal of Earth Sciences* 45: 83–98.

Johnson K and Smith DJ (2012) Dendroglaciological reconstruction of late-Holocene glacier activity at White and South Flat glaciers, Boundary Range, northern British Columbia Coast Mountains, Canada. *The Holocene* 22: 987–995.

Kobashi T, Severinghaus JP, Brook EJ, Barnola J-C, and Grachev AM (2007) Precise timing and characterization of abrupt climate change 8200 years agao from air trapped in polar ice. *Quaternary Science Reviews* 26: 1212-1222.

Koehler L and Smith DJ (2011) Late Holocene glacial activity in Manatee Valley, southern Coast Mountains, British Columbia, Canada. *Canadian Journal of Earth Sciences* 48: 603-618.

Lakeman TR, Clague JJ and Menounos B (2008) Advance of alpine glaciers during final retreat of the Cordilleran ice sheet in the Finlay River area, northern British Columbia, Canada. *Quaternary Research* 69: 188–200.

Larocque SJ and Smith DJ (2005) A dendroclimatological reconstruction of climate since AD 1700 in the Mt. Waddington area, British Columbia Coast Mountains, Canada. *Dendrochronologia* 22: 93–106.

Larsen CF, Motyka RJ, Arendt A, Echelmeyer K. and Geissler PE (2007) Glacier changes in southeast Alaska and northwest British Columbia and contribution to sea level rise. *Journal of Geophysical Research* 112: 1–11.

Lawson DE, Finnegan DC, Kopczynski SE and Bigl SR (2007) Early to mid-Holocene glacier fluctuations in Glacier Bay, Alaska. In: *Proceedings of the Fourth Glacier Bay Science Symposium* (eds Piatt JF and Gende SM), Juneau Alaska, 26-28 October 2004, pp.54-56. U.S. Geological Survey.

The Ledge (1912) The Ledge - The oldest mining camp newspaper in British Columbia. Greenwood, BC, Thursday March 21, 1912. Vol. XVIII: 1. Available at: http://historicalnewspapers.library.ubc.ca/view/collection/ledgreen/item/1309#1!Knipple (accessed 15 Aug 2014).

Luckman, BH (1995) Calendar-dated, early 'Little Ice Age' glacier advance at Robson Glacier, British Columbia, Canada. *The Holocene* 5: 149-159.

Luckman, BH (2000) The Little Ice Age in the Canadian Rockies. *Geomorphology* 32: 357-384.

Malcomb NL and Wiles GC (2013) Tree-ring-based reconstructions of North American glacier mass balance through the Little Ice Age - Contemporary warming transition. *Quaternary Research* 79: 123-137.

Mann M (2002) Little Ice Age in The Earth system: physical and chemical dimensions of global environmental change (Vol 1) in Encyclopedia of Global Environmental Change, MacCracken MC and Perry JS (eds.) pp 504-509. Chichester: John Wiley & Sons, Ltd.

Mathews H and Clague JJ (1993) The record of jokulhlaups from Summit Lake , northwestern British Columbia. *Canadian Journal of Earth Sciences* 30: 499–508.

Maurer MK, Menounos B, Luckman BH, Osborn G, Clague JJ, Beedle MJ, Smith R and Atkinson N (2012) Late Holocene glacier expansion in the Cariboo and northern Rocky Mountains, British Columbia, Canada. *Quaternary Science Reviews*. 51: 71-80.

Mayewski PA, Rohling EE, Stager JC, Karlen W, Maasch KA, Meeker LD, Meyerson EA, Gasse F, van Kreveld S, Holmgren K, Lee-Thorp J, Rosqvist G, Rack F, Staubwasserj M, Schneider RR and Steig EJ (2004) Holocene climate variabiliy. *Quaternary Research* 62: 243-255.

McKay NP and Kaufman DS (2009) Holocene climate and glacier variability at Gallet and Greyling Lakes, Chugach Mountains, south-central Alaska. *Journal of Paleolimnology* 41: 143-159.

Menounos B, Osborn G, Clague JJ, and Luckman, BH (2009) Latest Pleistocene and Holocene glacier fluctuations in western Canada. *Quaternary Science Reviews* 28: 2049–2074

Menounos B, Koch J, Osborn G, Clague JJ, and Mazzucchi D (2004) Early Holocene glacier advance, southern Coast Mountains, British Columbia, Canada. *Quarternary Science Reviews* 23: 1543-1550.

Menounos B, Clague JJ, Osborn G, Luckman BH, Lakeman TR and Minkus R (2008) Western Canadian glaciers advance in concert with climate change circa 4.2 ka. *Geophysical Research Letters* 35: 1–6.

Metcalfe P (2013) Technical Report on the Tide North Property, Stewart, British Columbia, Canada. Auramex Resource Group. pp 1-37.

Murton JP (1990) *Geophysical Report on an Airborne Magnetic VLF-EM SUS Stella, Rae, Linda & IWH 1-4 Claims*. Skeena Mining Division. Amphora Reseources. pp 1-39.

NOAA, National Oceanic and Atmospheric Administration (2014) User guide to COFECHA output files. NOAA Paleoclimatology. Available at: www.ncdc.noaa.gov/paleo/treering/cofecha/userguide.html#intercorrelation (accessed 07 July 2014).

Osborn G, Haspel R and Spooner I (2013) Late-Holocene fluctuations of the Bear River Glacier, northern Coast Ranges of British Columbia, Canada. *The Holocene* 23: 330-338.

Osborn G, Menounos B, Koch J, Clague JJ and Vallis V (2007) Multi-proxy record of Holocene glacial history of the Spearhead and Fitzsimmons ranges, southern Coast Mountains, British Columbia. *Quaternary Science Reviews* 26: 479–493.

Petrusiak JL (2012) *Late Holocene Activity at Scud Glacier*. BSc thesis, University of Victoria, Victoria, BC.

Pitman KJ and Smith DJ (2012) Tree-ring derived Little Ice Age temperature trends from the central British Columbia Coast Mountains, Canada. *Quaternary Research* 78: 417-426.

Porter SC and Denton GH (1967) Chronology of Neoglaciation in the North American Cordillera. *American Journal of Science* 265: 177–210.

Post A (1961) Austin Post collection. University of Alaska, Fairbanks, Geophysical Institute. Available at: http://www2.gi.alaska.edu/cgi-bin/gdftp/imageFolio.cgi (accessed 14 August 2014).

Ramsey BC and Lee S (2013) Recent and planned development of the program OxCal. *Radiocarbon* 55: 720-730.

Ramsey BC, van der Plicht J and Weninger B (2001) 'Wiggle matching' radiocarbon dates. *Radiocarbon* 43: 381-389.

Reimer PJ, Bailie MGL, Bard E, Bayliss A, Beck JW, Blackwell PG, Bronk Ramsey C, Buck CE, Burr GS, Edwards RL, Friedrich M, Grootes PM, Guilderson TP, Hajdas I, Heaton TJ, Kaiser KF, Kromer B, McCormac FG, Manning SW, Reimer RW, Richards DA, Suthon JR, Talamo S, Turney CSM, van der Plicht and Weyhenmeyer CE (2009) IntCal 09 and marine 09 radiocarbon age calibration curves, 0-50,000 years cal BP. *Radiocarbon* 51: 1111-1150.

Reimer PJ, Bard E, Bayliss A, Beck JW, Blackwell PG, Ramsey CB, Buck CE, Cheng H, Edwards RL, Friedrich RL, Grootes PM, Guilderson TP, Haflidason H, Hajdas I, Hatté C, Heaton TJ, Hoffman DL, Hogg AB, Hughen KA, Kaiser KF, Kromer B, Manning SW, Niu M, Reimer RW, Rinchards DA, Scott EM, Southon JR, Staff RA, Turney CSM and van der Plicht J (2013) IntCal13 and marine 13 radiocarbon age calibration curves 0–50,000 years cal BP. *Radiocarbon* 51: 1869-1887.

Reyes AV, Wiles GC, Smith DJ, Barclay DJ, Allen S, Jackson S, Larocque S, Laxton S, Lewis D, Calkin PE and Clague JJ. (2006) Expansion of alpine glaciers in Pacific North America in the First Millennium A.D. *Geology* 34: 57-60.

Rousse S, Kissel C, Laj C, Eriksson J and Knudsen K-L (2006) Holocene centennial to millennial-scale climatic variability: Evidence from high-resolution magnetic analyses of the last 10 cal kyr off North Iceland (core MD99-2275). *Earth and Planetary Science Letters* 242: 390–405.

Ryder JM (1987) Neoglacial history of the Stikine-Iskut area, northern Coast Mountains, British Columbia. *Candian Journal of Earth Sciences* 24: 1294-1301.

Ryder and Thomson (1986) Neoglacial in the southern Coast Mountains of British Columbia: Chronology prior to the late Neoglacial maximum. *Canadian Journal of Earth Sciences* 23: 273-287.

Schiefer E, Menounos B and Wheate R (2008) An inventory and morphometric analysis of British Columbia glaciers, Canada. *Journal of Glaciology* 54: 551–560.

Schmidt MW and Hertzberg JE (2011) Abrupt climate change during the last ice age. *Nature Education Knowledge* 3: 11.

Smith DJ and Laroque CP (1996) Dendroglaciologicl dating of a Little Ice Age glacial advance at Moving Glacier, Vancouver Island. *Géographie physique et Quaternaire* 50: 47–55.

Speer JH (2010) *Fundamentals of Tree-Ring Research*. Tuscon, AZ: University of Arizona Press.

Spooner IS, Mazzucchie D, Osborn G. and Larocque I (2002) A multi-proxy Holocene record of environmental change from the sediments of Skinny Lake, Iskut region, northern British Columbia, Canada. *Journal of Paleolimnology* 28: 419-432.

Steffen W, Crutzen PJ and McNeill JR (2007) The Anthropocene: Are humans now overwhelming the great forces of nature? *Royal Swedish Academy of Sciences* 36: 614-621.

Steinhilber F, Beer J, and Fröhlich C (2009) Total solar irradiance during the Holocene. *Geophysical Research Letters* 36: 1-5.

Stokes MA and Smiley TL (1968) *An Introduction to Tree-Ring Dating*. Chicago, IL: The University of Chicago Press.

Terasmae J (1961) Notes on late-Quaternary climate changes in Canada. *Annals of New York Academy of Sciences* 95: 658-675.

Tisdale EW, Fosberg MA and Poulton CE (1966) Vegetation and soil development on a recently glaciated area near Mount Robson, British Columbia. *Ecology* 47: 518-523.

Tomkins JD, Lamoureux SF and Sauchyn DJ (2008) Reconstruction of climate and glacial history based on a comparison of varve and tree-ring records from Mirror Lake, Northwest Territories, Canada. *Quaternary Science Reviews* 27: 1426–1441.

Untersteiner N and Nye JF (1968) Computations of the possible future behaviour of Berendon Glacier, Canada. *Journal of Glaciology* 7: 205-214.

USGS (2002) *Satellite Image Atlas of the World: Glaciers of North America*. U.S. Geological Survey Profession Paper 13-86. Richard WS Jr, and Ferringno JG (eds).

Vasskog K, Paasche Ø, Nesje A. Boyle JF and Birks HJB (2012) A new approach for reconstructing glacier variability based on lake sediments recording input from more than one glacier. *Quaternary Research* 77: 192-204.

Walker M (2005) *Quaternary Dating Methods*. West Sussex: John Wiley and Sons Ltd.

Wanner H, Beer J, Butikofer J, Crowley TJ, Cubasch U, Flickiger J, Goosse H, Grosjean M, Joos F, Kaplan JO, Kuttel M, Muller SA, Prentice IC, Solomina O, Stocker TF, Tarasov P, Wagner M and Widmann M (2008) Mid- to late Holocene climate change: An overview. *Quaternary Science Reviews* 27: 1791-1828.

Wiles GC, Barclay DJ, Calkin PE and Lowell TV (2008) Century to millenial-scale temperature vaiations for the last two thousand years indicated from glacial geologic records of southern Alaska. *Global and Planetary Change*. 60: 115-125.

Wilson RJS and Luckman BH (2003) Dendroclimatic reconstruction of maximum summer temperatures from upper treeline sites in Interior British Columbia, Canada. *The Holocene* 13: 851–861.

Winkler S and Matthews J (2010) Holocene glacier chronologies: Are "high-resolution" global and inter-hemispheric comparisons possible? *The Holocene* 20: 1137–1147.

Wright HEJ (1984) Sensitivity and response time of natural systems to climatic change in the late Quaternary. *Quaternary Science Reviews* 3: 91–131.

Zalasiewicz J, Williams M, Stefen W and Crutzen P (2010) The new world of the Anthropocene. *Environmental Science and Technology* 44: 2228-2231.

Appendix A: Methodology

This appendix describes the methodology used to anchor floating tree-ring chronology with a radiocarbon dated sample and explains the methods used to schematically depict chronologies (Figure 5.15). Floating chronology Bowser 6 will be used as an example.

Table A.1: The methods used for anchoring floating chronologies with radiocarbon dates are as follows:

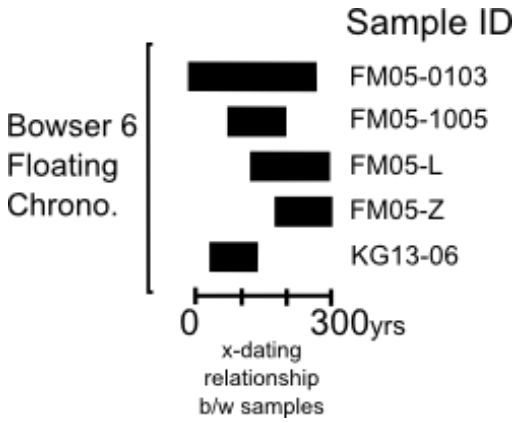	1. The samples are cross-dated into a floating chronology. The rectangles represent the temporal span of each sample based on the number of tree-rings.
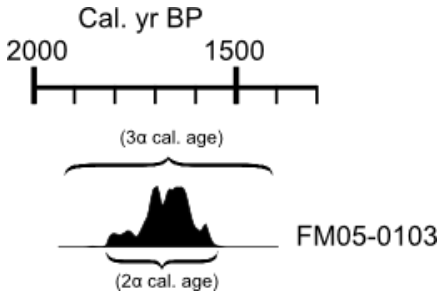	2. A sample is selected from the floating chronology to be radiocarbon dated. The conventional ^{14}C age of this sample is 1760±40 yr BP. Its 2α age is 1810-1560 cal. yr BP.
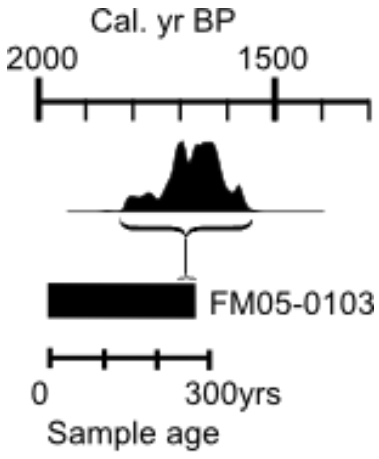	3. The radiocarbon age represents the age of the sample's perimeter wood. Standardized radiocarbon dating requires a ≥50g sample. Often this means that multiple rings from the perimeter are required to yield a single age.

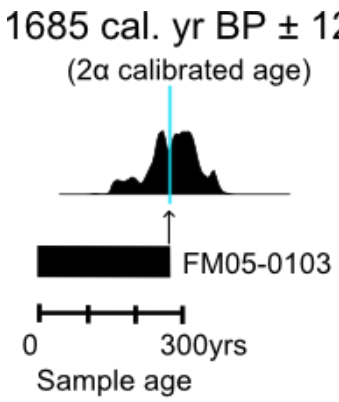	4. The mean of the 2α calibrated age range is selected to represent the age of the perimeter to avoid subjectivity associated with the 'wiggle-matching' method. The rationale for this is that wiggle-matching may not be appropriate for use in these samples, as the radiocarbon age is based on multiple rings.
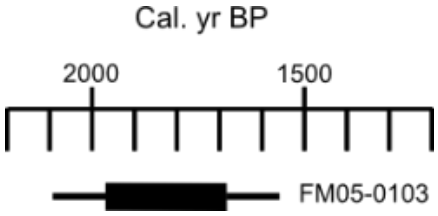	5. Bars are added to the radiocarbon dated sample based on the total 2α calibrated age range. Each bar is equal to the difference in total cal. age range divided by two. For this sample it would be (1810-1650)/2 =125 yr. These bars can be thought of as error bars, as they depict the possible range of years the tree may have lived in.
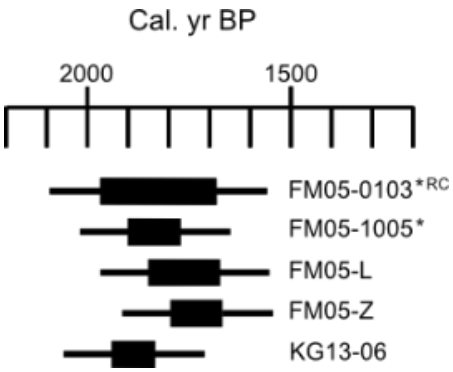	6. Because subsequent samples in the floating chronologies are cross-dated in relation to the radiocarbon dated sample, they receive error bars of the same magnitude. Symbols are added following sample id to denote the radiocarbon (RC) dated sample used for anchoring the chronology and in-situ (*) samples.

Appendix B: Results

Table B.1: Supplemental field and lab results. Bolded samples were those sent for radiocarbon dating to Beta Analytic Inc. Samples come from Charlie (KG), Canoe (CAN), Frank Mackie (FM), and Salmon (SG) glaciers. Tree species are either subalpine fir (SAF) or mountain hemlock (MH). Bolded samples were those sent for radiocarbon dating.

Glacier ID, Site #	Sample ID	Elev (m asl)	Location / Field Notes	Tree Species	In-Situ or Detrital (Sfc)	Internal x-date correl.
KG, S1	**KG13-01**	1080	Ice pressed between bedrock & till, standing upright, addition wood fragments pushed into till	SAF	In-Situ	0.515
KG, S1	KG13-02		Colluvial, in or on surface of lateral west lateral moraine south of KG13-01	SAF	Sfc	0.356
KG, S1	KG13-03		"	SAF	Sfc	0.460
KG, S1	KG13-04		"	SAF	Sfc	-
KG, S1	KG13-05		"	SAF	Sfc	-
KG, S1	KG13-06		"	SAF	Sfc	0.535
KG, S1	KG13-07		"	SAF	Sfc	0.610
KG, S1	KG13-08		"	SAF	Sfc	0.000
KG, S1	KG13-09		"	SAF	Sfc	0.000
KG, S1	KG13-10		"	SAF	Sfc	0.319
KG, S1	KG13-14		"	SAF	Sfc	-
KG, S1	KG13-15		"	SAF	Sfc	0.554
KG, S1	KG13-16		"	SAF	Sfc	0.000
KG, S1	KG13-17		"	SAF	Sfc	-
KG, S1	KG13-18		"	SAF	Sfc	-
KG, S1	KG13-19		"	SAF	Sfc	-
KG, S1	KG13-20		"	SAF	Sfc	-
KG, S1	KG13-21		"	SAF	Sfc	-
KG, S1	KG13-22		"	SAF	Sfc	0.070
KG, S1	KG13-23		"	SAF	Sfc	-
KG, S1	KG13-24		"	SAF	Sfc	-
KG, S1	KG13-25		"	SAF	Sfc	-
KG, S2	KG13-11		Over colluvium	SAF	Sfc	0.319

Table B.1 Cont.

KG, S2	**KG13-12**	977	Buried soil horizon- wood mat, pressed on Podzolic soil: Ae, B, C (orange)	SAF	In-Situ	-
KG, S2	KG13-13		Buried log on slope, left behind	SAF	?	-
KG, S2	KG13-27		Sticking out or gully side wall	SAF	Sfc	-
KG, S2	KG13-28		Over colluvium	SAF	Sfc	-
KG, S2	**KG13-29**	989	Buried perp. in gully, largest sample by far found at Charlie "Big Bertha"	SAF	In-Situ?	0.498
KG, S2	**KG13-30**	1040	Organic mat layer, 4m long bole	SAF	In-Situ	0.612
KG, S2	**KG13-31**	1040	Organic mat layer	SAF	In-Situ	-
KG, S2	KG13-32		In gully colluvium	SAF	Sfc	0.360
KG, S2	KG13-33		"	SAF	Sfc	-
KG, S2	KG13-34		"	SAF	Sfc	0.578
KG, S2	KG13-35		"	SAF	Sfc	0.451
KG, S2	KG13-36		"	SAF	Sfc	0.602
KG, S2	KG13-37		"	SAF	Sfc	0.640
KG, S2	KG13-38		"	SAF	Sfc	0.000
KG, S2	KG13-39		"	SAF	Sfc	0.781
KG, S2	KG13-40		"	SAF	Sfc	0.492
KG, S3	**KG13-26**	1228	Sticking out of distal side of lateral moraine, buried	SAF	In-Situ	0.690
KG, S3	KG13-26e		Extra piece broken off	SAF		-
KG. S4	**KG13-41**	873	Parameter wood sawed from SFC large bole below bedrock, additional samples (in-situ) pressed into bedrock cavities approx. ~10m above	SAF	Sfc	-
CAN, S1	**CAN06-01**		2nd wood mat horizon	MH	In-Situ	0.701
CAN, S1	CAN06-02		"	SAF	In-Situ	0.757
CAN, S1	**CAN06-03**		3rd wood mat horizon		In-Situ	-
CAN, S1	CAN06-11		"	SAF	In-Situ	0.530

Table B.1 Cont.

CAN, S1	CAN06-04		Surface/ on colluvium	MH	Sfc	0.483
CAN, S1	CAN06-05		"	MH	Sfc	0.574
CAN, S1	CAN06-06		"	SAF	Sfc	0.216
CAN, S1	CAN06-07		"	MH	Sfc	0.530
CAN, S1	CAN06-08		"	SAF	Sfc	0.660
CAN, S1	CAN06-09		"		Sfc	-
CAN, S1	CAN06-10		"		Sfc	0.400
CAN, S1	CAN06-12		"		Sfc	-
CAN, S1	CAN06-13		"	SAF	Sfc	0.517
CAN, S1	CAN06-14		"	SAF	Sfc	0.635
CAN, S1	CAN06-15		"		Sfc	0.551
CAN, S1	CAN06-16		"	MH	Sfc	0.583
CAN, S1	CAN06-17		"	MH	Sfc	0.223
CAN, S1	CAN06-18		"	MH	Sfc	0.618
CAN, S1	CAN06-19		"	SAF	Sfc	0.586
SG, S1	**SG13-01**		Buried beneath boulders in small pond, proximal to a small boulder moraine	MH	In-Situ	0.000
SG, S1	SG13-01e		Additional sample from same log as SG13-01	MH	In-Situ	0.000
FM, S1	FM05-0101	700	Gully Wall, Woody Layer (WL) 3		In-Situ	0.520
FM, S1	FM05-0102	700	Gully Wall, WL3		In-Situ	0.517
FM, S1	**FM05-0103**	700	Gully Wall, WL3	MH	In-Situ	0.656
FM, S1	**FM05-0104**	705	Standing upright in failure 'bowl',~ in line with WL2	MH	In-Situ	0.404
FM, S1	FM05-0105	705	Standing upright in failure 'bowl'	MH	In-Situ	0.728
FM, S1	FM05-0106	705	Standing upright in failure 'bowl'		In-Situ	0.214
FM, S1	FM05-0107	706	IN clay mound in centre Failure 'bowl'		In-Situ	0.520
FM, S1	FM05-0108	706	ON clay mound in centre Failure 'bowl'		Sfc	0.000
FM, S1	FM05-0109	708	N side of Failure 'bowl'		Sfc	0.276
FM, S1	**FM05-0110**	715	WL2 hanging @ top corner of gully wall/bowl	MH	In-Situ	0.265
FM, S1	FM05-0111	720	WL1 near top south side of failure bowl		In-Situ	0.516

Table B.1 Cont.

FM, S1	FM05-0112	720	WL1 near top south side of failure bowl		In-Situ	0.516
FM, S1	FM05-0113	720	WL1 near top south side of failure bowl		In-Situ	-0.141
FM, S1	FM05-0114	720	WL1 near top south side of failure bowl		Sfc	-0.034
FM, S2	FM05-01	817	Upper gully, moraines 1-3, main channel	MH	In-Situ	0.376
FM, S2	FM05-02	815	Upper gully, moraines 1-3, main channel	MH	In-Situ	0.456
FM, S2	FM05-03	815	Upper gully, moraines 1-3, main channel		In-Situ	-
FM, S2	FM05-04	813	Upper gully, moraines 1-3, main channel		In-Situ	0.421
FM, S2	FM05-05	815	Upper gully, moraines 1-3, WL4, below red clay		In-Situ	0.543
FM, S2	FM05-06	815	Upper gully, moraines 1-3, WL4, below red clay	MH	In-Situ	-
FM, S2	FM05-07	812	Upper gully, moraines 1-3, WL4, below red clay		Sfc	-
FM, S2	FM05-08	818	Upper gully, moraines 1-3, WL3, in red clay	MH	In-Situ	0.670
FM, S2	FM05-09	818	Upper gully, moraines 1-3, WL3, in red clay	SAF	In-Situ	0.429
FM, S2	FM05-10	819	Upper gully, moraines 1-3, WL3, in red clay	SAF	In-Situ	0.493
FM, S2	FM05-11	810	Upper gully, moraines 1-3, WL3, in red clay	MH	Sfc	0.515
FM, S2	FM05-12	816	Upper gully, moraines 1-3, WL3, in red clay	MH	In-Situ	0.664
FM, S2	FM05-13	808	Upper gully, moraines 1-3, lower down	MH	Sfc	0.692
FM, S2	FM05-14	807	Upper gully, moraines 1-3, WL3, in red clay	MH	Sfc	0.658
FM, S3	FM05-A	~580-680	South moraine complex, b/n camp and site 2	SAF	Sfc	0.548

Table B.1 Cont.

FM, S3	FM05-B	~580-680	South moraine complex, b/n camp and site 2	SAF	Sfc	0.408
FM, S3	FM05-C	~580-680	South moraine complex, b/n camp and site 2		Sfc	0.626
FM, S3	FM05-D	~580-680	South moraine complex, b/n camp and site 2		Sfc	0.518
FM, S3	FM05-E	~580-680	South moraine complex, b/n camp and site 2	MH	Sfc	0.232
FM, S3	FM05-F	~580-680	South moraine complex, b/n camp and site 2	SAF	Sfc	0.717
FM, S3	FM05-G	~580-680	South moraine complex, b/n camp and site 2		Sfc	0.638
FM, S3	FM05-H	~580-680	South moraine complex, b/n camp and site 2		Sfc	-
FM, S3	FM05-I	~580-680	South moraine complex, b/n camp and site 2	SAF	Sfc	0.519
FM, S3	FM05-J	~580-680	South moraine complex, b/n camp and site 2	SAF	Sfc	0.608
FM, S3	FM05-K	~580-680	South moraine complex, b/n camp and site 2		Sfc	0.454
FM, S3	FM05-L	~580-680	South moraine complex, b/n camp and site 2	MH	Sfc	0.428
FM, S3	FM05-M	~580-680	South moraine complex, b/n camp and site 2		Sfc	-
FM, S3	FM05-N	~580-680	South moraine complex, b/n camp and site 2		Sfc	-
FM, S3	FM05-O	~580-680	South moraine complex, b/n camp and site 2		Sfc	-
FM, S3	FM05-P	~580-680	South moraine complex, b/n camp and site 2		Sfc	0.460
FM, S3	FM05-Q	~580-680	South moraine complex, b/n camp and site 2		Sfc	0.154

Table B.1 Cont.

FM, S3	FM05-R	~580-680	South moraine complex, b/n camp and site 2		Sfc	-
FM, S3	FM05-S	~580-680	South moraine complex, b/n camp and site 2		Sfc	-
FM, S3	FM05-T	~580-680	South moraine complex, b/n camp and site 2		Sfc	-
FM, S3	FM05-U	~580-680	South moraine complex, b/n camp and site 2	MH	Sfc	0.499
FM, S3	FM05-V	~580-680	South moraine complex, b/n camp and site 2		Sfc	0.600
FM, S3	FM05-W	~580-680	South moraine complex, b/n camp and site 2	MH	Sfc	0.733
FM, S3	FM05-X	~580-680	South moraine complex, b/n camp and site 2		Sfc	-
FM, S3	FM05-Y	~580-680	South moraine complex, b/n camp and site 2		Sfc	0.120
FM, S3	FM05-Z	~580-680	South moraine complex, b/n camp and site 2	SAF	Sfc	0.647
FM, S3	FM05-AA	~620-700	South moraine complex, ~NW of Site 1		Sfc	-
FM, S3	FM05-BB	~620-700	South moraine complex, ~NW of Site 1		Sfc	0.287
FM, S3	FM05-CC	~620-700	South moraine complex, ~NW of Site 1	MH	Sfc	0.480
FM, S3	FM05-DD	~620-700	South moraine complex, ~NW of Site 1		Sfc	0.634
FM, S3	FM05-EE	~620-700	South moraine complex, ~NW of Site 1	MH	Sfc	0.742
FM, S3	FM05-FF	~620-700	South moraine complex, ~NW of Site 1		Sfc	-
FM, S3	FM05-GG	~620-700	South moraine complex, ~NW of Site 1		Sfc	-
FM, S3	FM05-GG	~620-700	South moraine complex, ~NW of Site 1		Sfc	-

Table B.1: Cont.

FM, S3	FM05-HH	~620-700	South moraine complex ~NW of Site 1		Sfc	0.505
FM, S3	FM05-II	~620-700	South moraine complex ~NW of Site 1		Sfc	-
FM, S3	FM05-JJ	~620-700	South moraine complex ~NW of Site 1		Sfc	0.447
FM, S5	**FM05-23**	757	Gully, north moraine wall		In-Situ?	0.881
FM, S5	**FM05-24**	755	Gully, north moraine wall, on organic mat		In-Situ	0.509
FM, S6	FM05-Nsfc01	~670-685	sfc below north morth moraines	MH	Sfc	0.639
FM, S6	FM05-Nsfc02	~670-685	sfc below north morth moraines	MH	Sfc	0.483
FM, S6	FM05-Nsfc03			MH	Sfc	0.594
FM, S6	FM05-Nsfc04				Sfc	-
FM, S6	FM05-Nsfc05			MH	Sfc	0.472
FM, S6	FM05-Nsfc06			MH	Sfc	0.000
FM, S6	FM05-Nsfc07				Sfc	-
FM, S6	FM05-Nsfc08			SAF	Sfc	0.497
FM, S6	FM05-Nsfc09			MH	Sfc	0.803
FM, S6	FM05-Nsfc10			SAF	Sfc	0.487
FM, S6	FM05-Nsfc11				Sfc	-
FM, S6	FM05-Nsfc12				Sfc	-
FM, S6	FM05-Nsfc13				Sfc	0.547
FM, S6	FM05-Nsfc14				Sfc	-
FM, S6	FM05-Nsfc15				Sfc	-
FM, S6	FM05-Nsfc16				Sfc	-
FM, S6	FM05-Nsfc17			MH	Sfc	0.689
FM, S6	FM05-Nsfc18			SAF	Sfc	0.514
FM, S6	FM05-Nsfc19			MH	Sfc	0.634
FM, S6	FM05-Nsfc20				Sfc	0.409
FM, S6	FM05-Nsfc21			MH	Sfc	-
FM, S6	FM05-Nsfc22				Sfc	0.586
FM, S6	FM05-Nsfc23			SAF	Sfc	-
FM, S6	FM05-Nsfc24				Sfc	-
FM, S6	FM05-Nsfc25			SAF	Sfc	-
FM, S6	FM05-Nsfc26			SAF	Sfc	0.619
FM, S6	FM05-Nsfc27			SAF	Sfc	0.526
FM, S6	FM05-Nsfc28			SAF	Sfc	0.536
FM, S6	FM05-Nsfc29				Sfc	0.000

Table B.2: Subfossil chronology results of Bowser 1-8. Ages anchored using radiocarbon dating. [1]Parameter age of the radiocarbon dated samples were assigned the mean calibrated radiocarbon age.

Floating Chronology Name	Sample ID.	Location (Glacier, Site #)	^{14}C age years, ± 2 sigma BP (Cal. yr BP)	Correlation with master	Number of rings	Perimeter Age (Cal. yr BP)[1]
Bowser 1	CAN06-11a	CAN, S1	4570 ± 40 BP* (5450-5050)	0.442	102	**5250**
	CAN06-11b			0.341	133	5248
	CAN06-07a	CAN, S1		0.410	100	5238
	CAN06-07b			0.357	102	5235
	CAN06-15a	CAN, S1		0.609	164	5280
	CAN06-15b			0.549	164	5210
Bowser 2	CAN06-01c	CAN, S1	3360 ± 40 BP* (3270-3470)	0.450	131	**3370**
	CAN06-01b			0.379	130	3369
	CAN06-04a	CAN, S1		0.498	56	3439
	CAN06-04b			0.585	54	3448
	CAN06-08a	CAN, S1		0.452	150	3377
	CAN06-08b			0.398	135	3392
	CAN06-13a	CAN, S1		0.333	144	3411
	CAN06-13b			0.468	138	3415
	CAN06-19a	CAN, S1		0.532	195	3417
	CAN06-19b			0.470	193	3420
Bowser 3	KG13-01c	KG, S1	3270 ± 30 BP (3570-3410)	0.523	59	**3490**
	KG13-01d			0.439	55	3494
	KG13-29b	KG, S3		0.286	140	3406
	KG13-29c			0.443	114	3432
	CAN06-02a	CAN, S1	3360 ± 40 BP** (3270-3470)	0.479	152	3358
	CAN06-02b			0.531	165	3345
	CAN06-16a	CAN, S1		0.493	65	3355
	CAN06-16b			0.466	64	3356
	FM05-26a	FM, S6		0.514	151	3227
	FM05-26b			0.452	133	3245
	FM05-27a	FM, S6		0.402	163	3254
	FM05-27b			0.409	178	3239
	FM05-28a	FM, S6		0.380	69	3372
	FM05-28b			0.451	70	3371

* Harvey et al., (2012). **Undated CAN06-02 was from same wood mat layer as radiocarbon-dated CAN06-01 and is assumed to be of similar age.

Table B.2: Cont.

Floating Chronology Name	Sample ID.	Location (Glacier, Site #)	^{14}C age years, ± 2 sigma BP (Cal yr BP)	Correlation with master	Number of rings	Perimeter Age (Cal yr BP)[1]
Bowser 4	KG13-30b	KG, S3	2620 ± 30 BP	0.498	123	2750
	KG13-30c		(2770-2730)	0.551	116	2757
	KG13-34a	KG, S3		0.414	172	2687
	KG13-34b			0.417	165	2693
	KG13-36a	KG, S3		0.458	141	2797
	KG13-36b			0.406	139	2799
	KG13-39a	KG, S3		0.359	113	2805
	KG13-39b			0.597	97	2821
	KG13-40a	KG, S3		0.480	69	2819
	KG13-40b			0.443	68	2820
Bowser 5	FM05-23a	FM, S5	2380 ± 40 BP	0.450	66	**2515**
	FM05-23b		(2690-2340)	0.460	60	2521
	FM05-24a	FM, S5	2490 ± 40 BP	0.446	87	2421
	FM05-24b		(2740-2370)	0.456	87	2421
	FM05-NSfc8a	FM, S6		0.433	84	2419
	FM05-NSfc8b			0.517	107	2394
	FM05-NSfc17a	FM, S6		0.494	191	2430
	FM05-NSfc17c			0.449	188	2434
	FM05-NSfc18a	FM, S6		0.242	121	2482
	FM05-NSfc18c			0.463	114	2487
	FM05-NSfc19a	FM, S6		0.487	175	2458
	FM05-NSfc19b			0.530	136	2497
	FM05-NSfc25a	FM, S6		0.451	129	2495
	FM05-NSfc25b			0.351	122	2502
Bowser 6	FM05-0103a	FM, S1	1760 ± 40 BP	0.403	276	**1685**
	FM05-0103d		(1810-1560)	0.492	194	1675
	FM05-0105a	FM, S1		0.400	112	1777
	FM05-0105b			0.597	96	1793
	FM05-La	FM, S3		0.345	152	1693
	FM05-Lb			0.488	168	1680
	FM05-Za	FM, S3		0.422	113	1673
	FM05-Zb			0.455	101	1685
	KG13-06a	KG, S1		0.434	81	1860
	KG13-06c			0.443	100	1841

Table B.2: Cont.

Floating Chronology Name	Sample ID.	Location (Glacier, Site #)	^{14}C age years, ± 2 sigma BP (Cal yr BP)	Correlation with master	Number of rings	Perimeter Age (Cal yr BP)[1]
Bowser 7	FM05-0104a	FM, S1	870 ± 40 BP (910-700)	0.327	187	**805**
	FM05-0104b			0.404	184	808
	FM05-CCa	FM, S3		0.341	145	773
	FM05-CCb			0.464	134	784
	FM05-NSfc1a	FM, S6		0.384	250	707
	FM05-NSfc1b			0.415	233	715
	FM05-NSfc2a	FM, S6		0.526	121	802
	FM05-NSFc2b			0.375	117	806
	FM05-NSfc5a	FM, S6		0.426	163	713
	FM05-NSfc5b			0.429	150	726
	FM05-01a	FM, S2		0.618	76	655
	FM05-01b			0.351	70	663
	FM05-02a	FM, S2		0.482	92	864
	FM05-02b			0.392	103	853
	FM05-11a	FM, S2		0.570	135	612
	FM05-11b			0.407	134	613
	FM05-12a	FM, S2		0.531	180	652
	FM05-12b			0.435	131	669
	FM05-13a	FM, S2		0.463	78	750
	FM05-13b			0.467	73	755
	FM05-14a	FM, S2		0.446	101	642
	FM05-14b			0.504	101	644
Bowser 8	KG13-26aa	KG, S2	470 ± 30 BP (540-500)	0.419	94	**520**
	KG13-26bb			0.514	99	516
	KG13-07a	KG, S1		0.501	64	477
	KG13-07b			0.433	99	448
	KG13-15a	KG, S1		0.491	143	442
	KG13-15b			0.436	162	424
	KG13-36a	KG, S3		0.362	141	482
	KG13-36b			0.463	139	484
	KG13-37a	KG, S3		0.532	91	538
	KG13-37b			0.473	105	524

Table B.3: Subfossil chronology results of Bowser 9 and 10. Samples are anchored to living tree chronologies from Surprise Glacier (Jackson et al., 2008)

Floating Chronology Name	Sample ID.	Location (Glacier, Site #)	Correlation with master	No. of rings	Perimeter Age (cal. yr BP)	Perim-eter Age (yr AD)
Bowser 9	FM05-09a	FM, S2	0.385	99	223	1727
	FM05-09b		0.478	99	223	1727
	FM05-Aa	FM, S3	0.418	107	155	1795
	FM05-Ab		0.475	106	156	1794
	FM05-Ba	FM, S3	0.336	127	177	1773
	FM05-Bb		0.404	111	192	1758
	FM05-Fa	FM, S3	0.484	139	123	1827
	FM05-Fb		0.652	123	137	1813
	FM05-Ia	FM, S3	0.442	164	135	1815
	FM05-IB		0.463	178	121	1829
	FM05-Jb	FM, S3	0.388	72	147	1803
	FM05-Ja		0.326	66	153	1797
	NSfc05-8a	FM, S6	0.344	84	170	1780
	NSfc05-8b		0.132	107	136	1814
	NSfc05-10a	FM, S6	0.494	58	143	1807
	NSfc05-10b		0.309	69	132	1818
	NSfc05-23a	FM, S6	0.334	113	141	1809
	NSfc05-23b		0.382	109	144	1806
Bowser 10	FM05-08a	FM, S2	0.518	65	230	1720
	FM05-08b		0.512	65	233	1717
	FM05-10a	FM, S2	0.394	36	235	1715
	FM05-10b		0.481	38	233	1717
	FM05-DDb	FM, S3	0.356	133	153	1797
	FM05-DDc		0.349	118	168	1782
	FM05-EEa	FM, S3	0.424	173	134	1816
	FM05-EEb		0.378	176	131	1819
	FM05-Ua	FM, S3	0.11	82	219	1731
	FM05-Ub		0.536	65	236	1714
	FM05-Wa	FM, S3	0.362	288	128	1822
	FM05-Wb		0.343	270	142	1808

Table B.4: Synthesis of radiocarbon ages from sites in the northern Coast Mountains. Ages have been calibrated with OxCal 4.2 InCal13 curve (Ramsey and Lee, 2013).

Lab No.	Sample ID	Reference	14C age (yr BP)	2σ calibration (cal. yr BP)	Description
Bear River Glacier, (55.56°N, 129.44°W)					
Beta-181857	BR03-801	Jackson et	3680 ±60	4200-3850	Wood in moraine
Beta-185808	BR03-806	al.(2008)	3340 ±60	3810-3410	Wood below moraine
Beta-180667	B3-03	Osborn et	3790 ±70	4410-3990	Wood mat 1, detrital
Beta-180666	B1-03	al.(2013)	3680 ±60	4220-3850	Wood mat 1, detrital
Beta-193482	B4B-04		3710 ±80	4350-3850	Wood mat 1, in situ
Beta-193483	B7-04		3540 ±60	3980-3650	Wood mat 2, in situ
Beta-195167	B9-04		3410 ±60	3850-3500	Gray till associtated with wood mat 3, detrital
Beta-193481	B3B-04		3380 ±60	3830-3480	Detrital wood
Beta-181861	B5-03		3330 ±60	3700-3410	Wood mat 3, detrital
Beta-193484	B8-04		3310 ±70	4800-3390	Gray till associtated with wood mat 3, I situ
Beta-193485	B10B-04		1040 ±50	1060-800	Wood mat 4, detrital
Berendon Glacier, (56.14°N, 130.06°W)					
TO-8975	BG-01	Clague et	3510+/-60	3966-3637	Twig from Berendon Pond
TO-8976	BG-02	al. (2004)	2710+/-60	2946-2747	Twig from Berendon Pond
TO-8977	BG-03		2700+/-60	2945-2742	Wood fragment from Berendon Pond
TO-9662	BG-04		1910+/-50	1971-2182	Wood fragment from Berendon Pond
TO-8978	BG-05		1780+/-50	1821-1569	Wood fragment from Berendon Pond
TO-4091	BG-06		720+/-50	735-558	Bark from Spillway Pond
LuA-5114	BG-07		615+/-85	702-508	Conifer fragment from Berendon Pond
TO-4152	BG-08		600+/-70	670-518	Abies needles from Spillway Pond
TO-4092	BG-09		520+/-60	654-484	Twig from Spillway Pond
LuA-5113	BG-10		505+/-80	663-325	Conifer fragment from Berendon Pond
TO-4090	BG-11		400+/-50	522-315	Twig from Spillway Pond
Bromley Glacier, (55.56°N, 129.44°W)					
Beta-310681	KHS1S1	Hoffman and	2470 ±30	2720-2380	Bole in moraine

Beta-310684	KHS3S1	Smith (2013)	2410 ±30	2690-2350	Detrital wood in think wood mat
Beta-310685	KHS2S6		1850 ±30	1865-1710	Log in creek bed
Beta-310682	KHS1S6		1480 ±30	1410-1300	In situ log in eroded gully, 50m below moraine crest
Beta-310683	KHS2S2		830 ±30	790-690	Log facing out in hard pack till
Canoe Glacier, (56.39°N, 130.06°W)					
Beta-242989	06CAN03	Harvey et	4570 ±50	5450-5050	Bole in moraine
Beta-242988	06CAN01	al. (2012)	3360 ±50	3710-3460	Log in moraine
Charlie Glacier, (56.27°N, 129.58°W)					
Beta-362278	KG13-01	This study	3270 ±30	3550-3410	Ice pressed between bedrock & till
Beta-362279	KG13-12		3260 ±30	3570-3400	Detrital wood found in wood mat over paleosol
Beta-362283	KG13-41		3230 ±30	3560-3380	Surface, detrial log
Beta-362281	KG13-30		2620 ±30	2880-2730	Organic mat layer
Beta-362282	KG13-31		2460 ±30	2710-2380	Organic mat layer
Beta-362280	KG13-26		470 ±30	540-490	Sticking slightly out of distal side of lateral moraine
Forrest Kerr Glacier, (56.10°N, 129.34°W)					
Beta-197981		Lewis and	1780 ±60	1860-1560	Exhumed in situ stump, direct age
Beta-197980		Smith (2005)	1720 ±50	1800-1530	Exhumed in situ stump, direct age
Beta-197979			1690 ±50	1720-1430	Exhumed in situ stump, direct age
Beta-197977			1490 ±60	1520-1300	Wood in till, max age
Beta-242984	FK06-06a	UVTRL subfossil	1670 ±50	1710-1410	
Beta-242982	FK06-04a	database,	1670 ±50	1710-1410	
Beta-242986	FK06-04b	Unpublished	1630 ±50	1690-1400	
Beta-242985	FK06-01b		1600 ±50	1610-1380	
Beta-242983	FK06-05a		1570 ±50	1550-1390	
Frank Mackie Glacier, (56.33°N, 130.11°W)					
Beta-217006	FM-L3	This study	2380 ± 40	2690-2330	Gully, north moraine wall

Beta-217007	FM-L4		2490 ± 40	2740-2380	Gully, north moraine wall, on organic mat
Beta-242990	FM05-03a		1760 ± 40	1810-1570	Gully wall
Beta-242991	FM05-04		870 ± 40	910-690	Failure 'bowl', upright
Beta-242992	FM05-10		860 ± 40	900-690	Hanging at top corner of gully wall/bowl
Beta-242994	FM05-06b		560 ± 50	650-510	Failure 'bowl'
Glacier B, (57.04°N, 131.02°W)					
S-2296		Ryder (1987)	595 ±60	660-520	Ah material from paleosol
Juneau Icefield: Llewellyn and Tulsequah glaciers, (59.03°N,133.58°W)					
AA46376		Clague et al. (2010)	1272 ±52	1290-1070	Pith of glacially overridden tree, tree stem
Beta-200739			1210 ±40	1260-1010	Early LIA lake, twig
Beta-200841			1000 ±50	1050-790	Maximum age for glacier advance, branch or root
Beta-200740			980 ±40	960-790	Max age for glacier advance, tree stump
UCIAMS-45009			950 ±15	920-800	Glacier advaning, tree stump
GSC-6632			930 ±40	930-760	Max age for glacier advance, branch in till
GSC-6630			820 ±70	910-660	Glacier advaning, tree stump
GSC-6634			780 ±70	900-560	Glacier advaning, tree stump
AA54469			454 ±37	540-340	LIA lake, twig
Salmon Glacier, (56.16°N,130.08°W)					
Beta-362277	SG13-01	This study	4950 ±30	5740-5610	Buried under moraine in pond
Scud Glacier, (57.18°N, 131.21°W)					
Beta-242979	SD06-43	UVTRL subfossil	2760 ±60	3000-2760	In situ log
Beta-242981	SD06-52	database,	1540 ±70	1540-1330	Log in moraine
Beta-242577	SCD06-15	Unpublished	900 ±50	930-730	
Beta-242978	SCD06-18		900 ±40	920-730	
Beta-242976	SD06-15		880 ±50	910-700	
Beta-242981	SD06-44		80 ±50	270-10	

S-2298		Ryder(1987)	625 ±140	900-320	Tree in growth position
S-2297			455 ±65	630-310	Tree in growth position
South More Glacier					
Beta-217008	MG05-NCl	Craig et al. (2011)	1490 ±50	1520-1300	Subfossil boles and stumps
Surprise Glacier(56.26°N, 129.75°W)					
Beta-181858	SG03-801	Jackson et al. (2008)	2960 ±70	3350-2930	Lateral moraine
Beta-197984	SG04-8S8		1690 ±60	1730-1410	Lateral moraine
Beta-197983	SG04-829		1610 ±50	1610-1390	Lateral moraine
Beta-197986	SG04-804		1440 ±60	1520-1270	Lateral moraine
Tide Lake, (56.30°N, 130.06°W)					
GSC-1372	TL-01	Clague and Mathews (1992)	2730 ±170	3330-2370	Wood, lake sediments, from drill hole 45m below surface
TO-2205	TL-02		2700 ±60	2910-2740	Conifer needles, from drill core 53m below surface
TO-22-04	TL-03		2650 ±60	2920-2540	Conifer needles, from drill core 42-45m below surface
GSC-5349	TL-04		1640 ±60	1700-1400	Log, from exposed fluvial or glaciofluvial gravel
TO-2898	TL-05		1600 ±40	1570-1390	Conifer needles from exposed deltaic sand exposed
GSC-5386	TL-06		1520 ±50	1530-1320	Wood fragment, from exposed glaciolacustrine mud
TO-2897	TL-07		1440 ±40	1400-1290	Wood fragment from exposed glaciolacustrine mud
GSC-5305	TL-08		990 ±60	1050-760	Log from glaciolacustrine mud exposed in river bluff
TO-4975	TL-09		710 ±50	730-550	Branch from glaciolacustrine mud exposed in river bluff
TO-2203	TL-10		520 ±60	650-450	Conifer needles, drill core 8m below surface
GSC-5336	TL-11		520 ±60	650-450	Branch from glaciolacustrine mud exposed in river bluff

Todd Valley Glaciers, (56.19°N, 129.70°W)					
Beta-181859	TG03-806	Jackson et	2300 ±60	2490-2150	Bole in lateral moraine
Beta-199708	TG04-874	al. (2008)	1690 ±60	1730-1410	Bole in lateral moraine
Beta-181560	TG03-815		1540 ±60	1550-1320	Outwash deposit
Beta-197989	TG04-805		730 ±60	780-550	Log buried in till
Beta-197990	TG04-838		660 ±60	690-540	In growth position
Beta-197991	TG04-871		660 ±60	690-540	In growth position
Beta-197986	TG04-801		450 ±60	630-320	log in lateral moraine
Beta-208442	TG04-872		410 ±60	530-310	log in lateral moraine
Beta-208443	TG04-879		360 ±60	510-300	log buried in till
Beta-197987	TG03-802		160 ±60	-	Glacier killed tree
White and South Flat Glaciers (55.49°N, 129.28°W)					
Beta-262877	WG02-03	Johnson and	1550 ±40	1530-1360	Wood in moraine
Beta-262878	WG03-14	Smith (2012)	1530 ±50	1530-1320	Detrial wood
Beta-262876	WG01_01		1460 ±40	1470-1290	Wood in moraine
Beta-262879	WG05-02		1400 ±40	1380-1270	Wood in moraine
Beta-250505	WG06-04		1360 ±50	1350-1180	Detrial wood
Beta-273508	WG03-10		1360 ±40	1340-1180	Wood in moraine
Beta-250501	WF07-01		1280 ±50	1290-1070	Lake sediments
Beta-273508	WG08-12		960 ±40	950-790	Lake sediments
Beta-250503	WG09-16		810 ±40	790-670	Lake sediments
Beta-250504	WG09-18		610 ±60	670-530	Lake sediments